

Jukka Juntti

**Simulation of passive radar for air surveillance scenario
training system**

Master's Thesis in Information Technology

March 25, 2021

University of Jyväskylä

Faculty of Information Technology

Author: Jukka Juntti

Contact information: jukka.juntti@gmail.com

Supervisors: Timo Hämäläinen, and Hannu-Heikki Puupponen

Title: Simulation of passive radar for air surveillance scenario training system

Työn nimi: Passiivisen tutkan reaaliaikainen simulointi ilma-
valvonnan harjoittelujärjestel-
mässä

Project: Master's Thesis

Study line: Information technology

Page count: 76+0

Abstract: Passive radars are an increasingly interesting type of radar for modern air surveillance systems. In this thesis, development of real-time simulation model for passive radar is studied considering design, implementation and evaluation. Methodologically this research is approached with combination of design research and simulation study, together forming a framework for design in model conceptualisation. To support the design efforts, a theoretical background is provided by literature review of basic radar concepts followed by historic and modern research on passive radars. An abstract model is described in UML notation that encapsulate components of passive radar and using the model a scheme for simulated signal processing is proposed as an evaluation for the model, which is then implemented into an air surveillance training simulation. This simulation implementation was compared to existing research depicted in literature review. Results show that the simulation is capable of depicting basic passive radar performance such as maximum range, integration gain and effects of signal-to-interference ratio and serves as an effective base for more sophisticated design.

Keywords: real-time, simulation, passive radar, air surveillance, training system

Suomenkielinen tiivistelmä: Passiiviset tutkat ovat kasvava kiinnostuksen kohde ilma-
valvonnan sovelluksiin. Tässä tutkielmassa perehdytään passiivisen tutkan reaaliaikaiseen simu-
lointiin suunnittelun, implementoinnin ja evaluoinnin näkökulmasta. Työ alkaa esityksellä

suunnittelutieteen soveltumisesta simulaation kehitykseen verraten näiden vaiheita ja yhtenevyyksiä, jonka pohjalta esitellään viitekehys simulaation suunnittelututkimukseen. Passiivisen tutkan teoria muodostetaan tutustumalla tutkateorian käsikirjoihin sekä kirjallisuuskatsauksella aikaisempaan tutkimukseen. Tutkielman tuloksena esitellään simulaatiomalli passiiviselle tutkalle, jonka pohjalta kehitetään referenssitoteutus simuloidulle signaalinkäsittelylle ja havainnontuotolle. Simulaation validoidaan rakentamalla aikaisemman tutkimusten passiivisia tutkia simulaatioskenaarioihin ja vertailemalla simuloitua suorituskykyä. Tulokset osoittavat, että simulaatio pystyy mallintamaan passiivisten tutkien yksinkertaisia ominaisuuksia kuten maksimi kantama, integraation vahvistus ja signaali-interferenssin vaikutus.

Avainsanat: reaaliaikainen, simulaatio, passiivinen tutka, ilmavalvonta, harjoitusjärjestelmä

Glossary

ADC	Analog-to-digital converter
ADS-B	Automatic Dependent Surveillance–Broadcast
DAB	Digital Audio Broadcasting
DRM	Digital Radio Mondiale
DVB-T	Digital Video Broadcasting, Terrestrial
DSR	Design Science Research
FM	Frequency Modulated
GLONASS	Global Navigation Satellite System
GNSS	Global Navigation Satellite System
GPS	Global Positioning System
GSM	Global System for Mobile Communications
JSON	Javascript Object Notation
LTE	Long Term Evolution
PCL	Passive Coherent Location
PBR	Passive bistatic radar
RCS	Radar cross section
SNR	Signal-to-noise ratio
SIR	Signal-to-interference ratio
UMTS	Universal Mobile Telecommunications System
WiMAX	Worldwide Interoperability for Microwave Access
WTC	Wake Turbulence Category

List of Figures

Figure 1. Steps of simulation development.	7
Figure 2. Design cycles in Takeda framework.....	9
Figure 3. Simulation design science research.	11
Figure 4. Simulation execution.....	14
Figure 5. Basic monostatic radar.	18
Figure 6. Detection threshold example.	19
Figure 7. Simple passive radar example.	22
Figure 8. Target position in bistatic detection.	23
Figure 9. Target location with triangulation.	24
Figure 10. Radiation pattern of half-wave dipole antenna in 2D.....	28
Figure 11. Radiation pattern of half-wave dipole antenna in 3D.....	28
Figure 12. Passive radar model architecture overview in UML.....	38
Figure 13. Passive radar components and their relation to model.....	39
Figure 14. Gain table mesh into sphere transform.	41
Figure 15. Radiation pattern of antenna used in PBR 6, 7 and 8.	50
Figure 16. Overview of first simulation run setup.....	52
Figure 17. Comparison of SNR to Pd value between simulation results and theoretical assumption.....	54
Figure 18. PBR 1 detections of few selected targets.	55
Figure 19. PBR 2 and PBR 3 detections of few selected targets.	56
Figure 20. PBR 4 detections of all targets.	57
Figure 21. Detection results of second test scenario.	58
Figure 22. Comparison to results of (Xie et al. 2018).....	59
Figure 23. PBR 9 detections of few selected targets.	60
Figure 24. PBR 10 detections of all targets.....	61
Figure 25. Improved model based on suggestions.	64

List of Tables

Table 1. IEEE Std 521-1984 Radar frequency band nomenclature.....	21
Table 2. Gain table demonstration.	40
Table 3. Radar configurations in the test scenarios.....	49
Table 4. Illuminator configurations in the test scenarios.	49
Table 5. Gain table of a single antenna element used in PaRaDe (PBR 1, 2 and 3).	49
Table 6. Gain table of surveillance antenna array used in the PBR 4.	50
Table 7. Gain table of the 4 element yagi antenna used in the PBR 5.....	50

Contents

1	INTRODUCTION	1
2	METHODOLOGY	3
	2.1 Simulation study.....	3
	2.2 Design science reserach	8
	2.3 Framework for design	10
3	DISCRETE EVENT SIMULATION	13
	3.1 Reference architecture	14
	3.2 Target position representation	15
4	INTRODUCTION TO RADAR.....	17
	4.1 Basic radar operation.....	17
	4.2 Passive bistatic radar	21
	4.3 Antenna properties	27
	4.4 Passive radar demonstrations in research	29
	4.5 Illuminator	34
5	PASSIVE RADAR MODEL CONCEPTUALISATION	37
	5.1 Passive radar components.....	37
	5.2 Antenna gain.....	39
	5.3 Execution overview	42
	5.4 Pre-processing detection candidates.....	42
	5.5 Simulated signal processing	43
	5.5.1 SNR calculation.....	44
	5.5.2 Physical shielding.....	44
	5.5.3 Integration gain	45
	5.5.4 Probability of detection and false alarm	45
	5.6 Model translation	45
6	VERIFICATION & VALIDATION.....	46
	6.1 Target data	46
	6.2 Radar & illuminator configuration	47
7	RESULTS	51
	7.1 Test simulation analysis	51
	7.1.1 First test scenario	51
	7.1.2 Second test scenario	58
	7.1.3 Third test scenario	59
	7.2 Problems and suggestions.....	61
	7.3 Improved model	63
8	CONCLUSION	65

BIBLIOGRAPHY 66

1 Introduction

Radar is an electromagnetic system for detecting aircraft, land vehicles, ships and other objects in space or nature. Radar systems play important role in air surveillance. Providing accurate positioning and tracking of multiple aircraft which is essential for effective air traffic control in commercial aviation as well as national airspace surveillance. (Skolnik 2001)

In this paper the definition of radar is separated in two main categories: active radars and passive radars. Active radar is composed of two co-operating key radar components, transmitter and receiver in same or separate locations, while passive radars have a receiving component and uses reflections from known non co-operative sources. The concept of passive radar and its performance metrics are discussed more thoroughly in chapter 4.

Although the concept of passive radar dates back to the very first experiments of a radar system (Melvin 2014), and seconds world war (Griffiths and Willis 2010), the interest in passive radar development has increased in past few decades. Compared to common monostatic radars bistatic and multistatic radars are performing better when detecting stealth aircraft (H. D. Griffiths and C. J. Baker 2017). Passive radars do not have a transmitter and therefore do not radiate, which makes passive radars ideal in populated areas, such as busy city centers and airports to provide additional surveillance information of the airspace. Passive radars are also practically immune to anti-radar systems and directional jamming. (H. D. Griffiths and C. J. Baker 2017)

Simulation training is key component in air surveillance training, it makes learning the concept of used equipment and technology possible without the need of acquiring any products. Earlier research to real-time simulation of passive radar is done by (Zywek, Malanowski, and Baczyk 2016), where a signal processing and plot simulation was developed with randomly and dynamically generated targets utilising ADS-B exchange flight data. Simulation in general is widely used to predict the performance a developed passive radar (Sun, Tan, and Lu 2008), (Pölönen and Koivunen 2013), (Malanowski and Kulpa 2008), (Petó et al. 2014), (Guo, Woodbridge, and Baker 2008), (Xianrong et al. 2011).

This research studies the development of passive radar simulation model for real-time sim-

ulation. The main research question of the research is: *how to model a passive radar for real-time simulation?* In chapter 3, a framework for design of simulation is presented and analyzed.

Simulation model design is dependent on the end use and model designer(s) need to go through tradeoffs concerning efficacy and fidelity, so that the end result will satisfy the goals (Barott, Dabrowski, and Himed 2015). For air surveillance training system that is running in real time, the simulation model should be able to produce realistic results in short time periods. Earlier research on passive radar simulation has little to no guidelines or strategies for tradeoff choices. In addition to answering main research question, the second goal of this research is to identify and rank suitable tradeoffs for real-time passive radar simulation.

Applying general theory of passive radar research from literature discussed in chapter 4 and development guidelines lined out in chapter 2 and chapter 3, a simulation model for real-time passive radar is introduced in chapter 5. The simulation model is evaluated by implementing it into training simulation and measured for its performance and utility. Evaluation process and used test cases are described in chapter 6. The implementation used in performance analysis is not open source. For readers, a reference architecture of the model along with execution steps of the developed processing scheme is provided. Results of testing the model are presented in chapter 7. Analysis of the results with implications, conclusions and future research are discussed in chapter 8.

2 Methodology

In this chapter we formulate the research methodology followed in this research. It starts with by describing principles of simulation study and pointing out the relevant parts for passive radar simulation model construction followed by reviewing design research methods applicable for simulation design. The simulation study in this research follows guidelines for simulation study introduced by (Banks et al. 2005) and propose a recipe for the model conceptualisation for passive radar. Simulation theory applied in this research is discussed in chapter 3. A framework for design is introduced in section 2.3.

2.1 Simulation study

The research method of this research goes partially by following the simulation study method described in (Banks et al. 2005) and applying some aspects of design science research. Principles of design science are applied in the Model Conceptualisation phase where the recipe for passive radar simulation is proposed through iterative development of the simulation model. In this section we will shortly describe the phases of simulation study and how they are carried out in this research.

Guidelines introduced in (Banks et al. 2005) describe process of simulation development in 12 steps:

1. Problem formulation
2. Setting of objectives and plans
3. Model conceptualisation
4. Data collection
5. Model translation
6. Verification
7. Validation
8. Experimental design
9. Production runs and analysis
10. Evaluation of runs

11. Documentation and reporting

12. Implementation

The steps and transitions between them are illustrated in Figure 1. In this research the main focus is the model construction phase highlighted in green.

Final step implementation, is not actual single step and more of a meta-step that combines the whole 11 steps and their success (Banks et al. 2005). All the 12 phases can be divided in four main phases of the simulation study: Formulation phase (steps 1 and 2), Model construction phase (steps 3 to 7), Experiment phase (steps 8 to 10) and Implementation phase (steps 11 and 12) (Banks et al. 2005).

According to (Banks et al. 2005), the whole process should start with stating the problem at hand: what is this simulation for? This can be thought as the formulation of a business need for the simulation, there is a business problem and simulation is chosen to be answer to the problem. The original problem that led to this research was: *we want to simulate passive radar in air surveillance training system.*

Setting of objectives and plans draws boundaries and gives scope to the simulation study. Objectives describe questions the simulation should bring answers to and planning includes effort estimates and resource management of the project concerning costs and project team management (Banks et al. 2005). In this research, this step is essentially done and reported in the introduction chapter. The objective is to achieve simple, yet effective model for passive radar simulation.

The cyclic development of the simulation model begins with *Model conceptualisation* together with *data collection*. Model conceptualisation is the step where the real system or phenomenon is constructed into a set of abstract objects, a model that can later be turned into a software. According to (Banks et al. 2005) the construction of simulation models is "as much art as science", meaning that there are so many ways to approach abstraction of real world systems and phenomena. There are general guidelines for building successful models that include basic instructions such as starting from lower complexity and gradually increasing towards a more sophisticated model. Model conceptualisation in this research is described in more detail in chapter 5.

Data collection step is responsible for gathering correct input and output data for verification and validation. Data collection is meant to be performed while constructing the model for two main reasons according to (Banks et al. 2005): first, data collection should be started as early as possible since long history of data ensures better representation of input data that can be fed to the simulated system. Secondly, as the model concept grows in complexity over the course of development, so can the required data, which in turn with the first reason should begin early. In data collection step both, input data and verifying output data is collected.

In this research, there are two main categories of data to be collected: target data and reference data of passive radar performance, where target data is the main input data and performance reference data is used to validate the model. Target data can be manually generated by hand or parsed from flight data provided by various services like ADS-B Exchange. Performance reference data is collected by extracting results of various existing research on passive radar demonstrators.

Model translation is the step where the simulation model is translated to language that can be run in a computer as software (Banks et al. 2005). Simulation software evolves and changes fast as any other software over time and there are multiple options to consider when choosing the underlying programming language for the simulation model translation. Depending on resources, experience and the model, the simulation can be developed "from scratch" by using fairly low level general purpose programming languages such as Java or C++ but there exists plethora of both, commercial and free, simulation software that require little to no code at all. Ultimately, it is up to the simulation developer to justify and recognise the suitable approach (Banks et al. 2005).

In this research for the model translation it was decided very early on that the implementation is done by using Java. There are two reasons to back up this decision. First, the context the simulation research was first introduced; *there exists a system (written in Java) that could benefit from simulation model for passive radar*. Second, the developer of the model has the most experience in Java and integration of the model into the system for validation and verification benefits from common technology.

Purpose of verification step is to ensure correct execution in the software. Verification of the

model is essentially a system verification of the simulated model in the software and making sure there are no "bugs" in the translation (Banks et al. 2005). For this research, verification of the model consists of programming paradigms used in Java development, utilizing unit tests. Verification also includes manually calculating few random samples of simulation events and comparing results to that of simulation runs. Once the translated model is verified the validation step begins.

Validation step tests the conceptualised model by comparing the simulated system behaviour and results to a known system. These results are analysed and a new cycle is started in hopes of improving the model. (Banks et al. 2005).

Rest of the steps, experimental design, evaluation of runs, documentation and reporting are out of scope of this research. Experimental design comes after the model is validated and taken into use in the system and executed in multiple runs which are then analysed. Since the end system where the model will be used after the research is a training system, it could be entirely another research subject to examine how well the simulation model improves the training.

In this research the main focus is the model construction phase highlighted in Figure 1

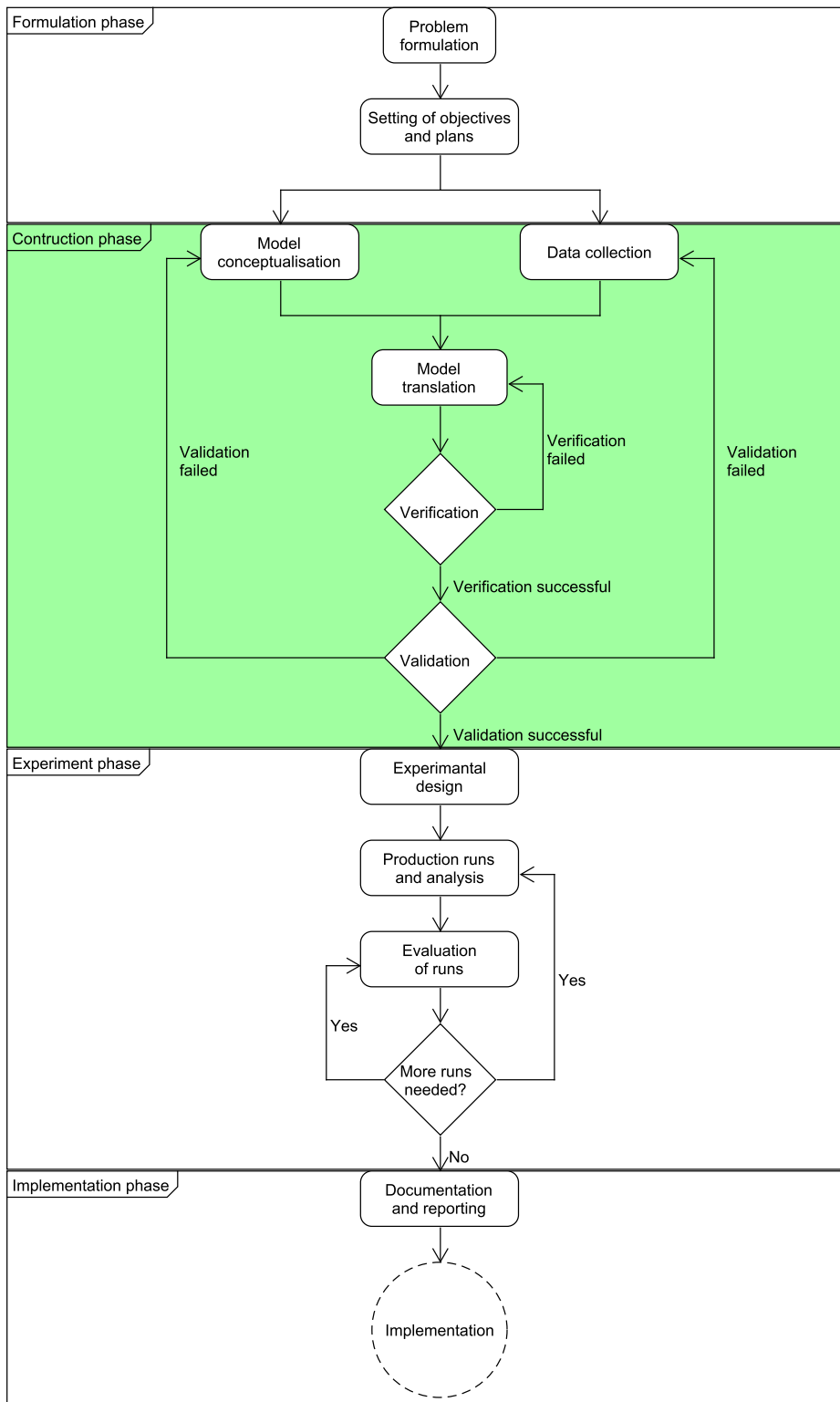


Figure 1. Steps of simulation development.

2.2 Design science reserach

Design science research (DSR) is a research methodology about design and construction of *artifacts* and theory of design. DSR process yields an artifact or multiple artifacts whose purpose is to answer research questions, bring knowledge and improve existing practises of the domain in which the artifact is used. Artifacts include abstract concepts like architectures, frameworks, models, constructs, design principles, theories and methods as well as instantiations which are concrete manifestations of artifacts. (Vaishnavi, Keuchler, and Petter 2019)

The core of design science research method is a some form of a design cycle. A good starting point to describe and visualise cognitive process of a design cycle is described by (Takeda et al. 1990). The process is divided to four sections: formulation of problem, suggestion and development, evaluation and conclusion, where conclusion section is the terminal phase. Illustrated process in Figure 2.

First step is becoming aware of the problems in the current design (or the complete lack of it) and create set of specification the design should fulfill. In this research the initial step is motivated by the first step of simulation study described earlier in section section 2.1. After the problems are formulated design work begins by making suggestions to resolve those problems.(Takeda et al. 1990)

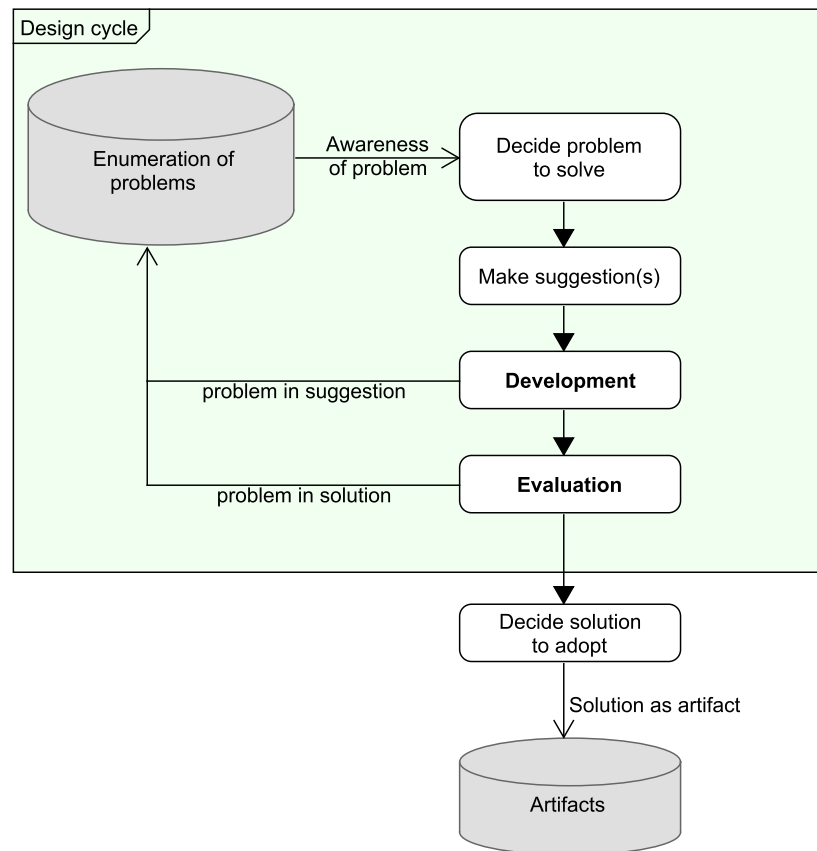


Figure 2. Design cycles in Takeda framework.

A tentative design is developed based on the suggestions to provide solution to the problems. Development is essentially the construction of the artifact which can either be an abstract design or an instantiation of some more general design. After development the design is evaluated for its ability to provide a solution to the problem. In both, development and evaluation phase, the designer can encounter a new problem and the process falls back to the awareness of a problem phase and restarting the cycle. (Takeda et al. 1990)

Problems revealed in development phase are caused by lack of information. This means that due to inexperience of the problem domain, the suggestion to the original problem was hiding another problem that was revealed when the suggestion was being implemented. These problems are solved by getting the missing information (if it is possible). Problems from evaluation phase are caused by contradictions in the theory due to incompleteness. An an-

swer to the contradiction problems in theory are dealt with circumscription which is essentially reformulating the theory of the cycles design.(Takeda et al. 1990)

Conclusion phase is not described as a specific sub-process of the framework (Takeda et al. 1990). Conclusion phase is gathering information and making decisions based on the design cycles on what solutions to adopt into the design.

2.3 Framework for design

Adopting the design research framework described in (Takeda et al. 1990) and simulation construction (Banks et al. 2005) we merge the phases between the two to get a framework for simulation design research which is illustrated in Figure 3.

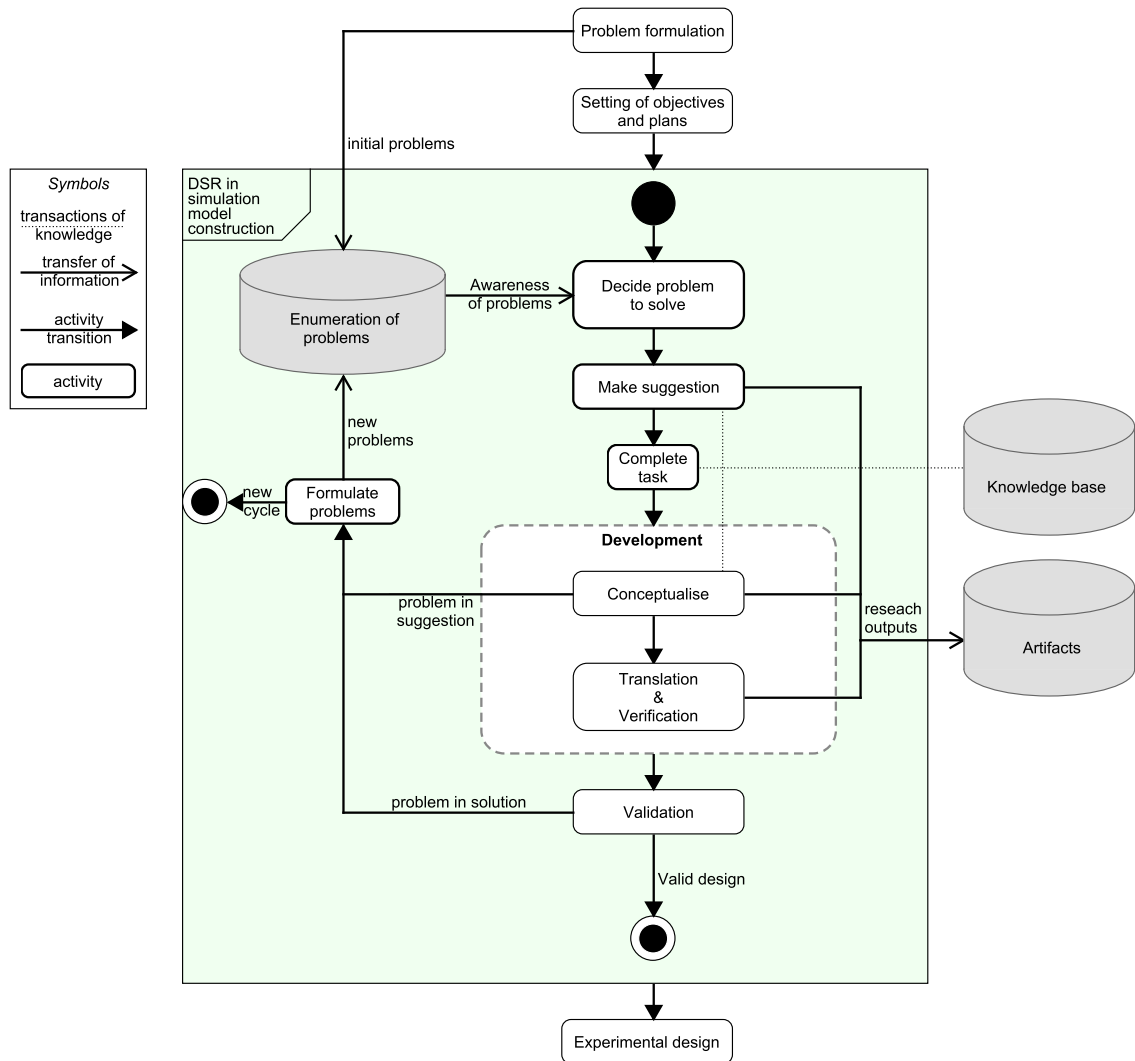


Figure 3. Simulation design science research.

The problem formulation gives the initial problems to the simulation construction cycles. Initial problems include problems that are very general and solutions to these might not be answered in development at all but instead in a task. Tasks are rudimentary activities like finding general information on a subject and submitting it into the knowledge base. Issues revealed in the validation feed back to the design cycles as new problems which will be solved in the following design cycles.

Suggestion, conceptualisation and translation contribute to the research outputs (i.e. artifacts). Suggestions can be evaluated to reveal their contribution to the overall development

process in terms of feasibility and effectiveness. Suggestions to approach certain problem and how to solve it are essentially based on intuition and the added value is not certain. Evaluating suggestions yield guidelines for good practises and frameworks for design. Even the framework adopted in this chapter is under scrutiny at conclusion sections chapter 8. Model conceptualisation yields abstract artifacts: models, architectures and theory. Model translation outputs an instantiation of the simulation model which is a software.

Validation represents the evaluation of design science research. The constructed artifacts (model and its instantiation) are evaluated against the set of criteria that define "good enough" requirements for the simulation.

Existing knowledge is used when problems are analysed and suggestions made or new solutions are developed. Transactions of knowledge happen when new or updated information is presented to the knowledge base.

3 Discrete event simulation

Before designing and constructing the simulation model, the environment for the model needs to be described. This chapter introduces definitions and terminology used in discrete real-time simulation development and describes the reference simulation system and architecture for which the developed model will be implemented in.

Simulation is an imitation of a system or phenomenon of real world. It is defined through a set of instructions or rules of interaction between entities across time, called a *model*. Simulation is used to answer to problems, that can be described mathematically but are too complex to be solved analytically. When there are too many variables and relationships between entities, it is more feasible to let computer run calculations of the many interactions. This allows studying a system for its performance in various scenarios without actually building the system. (Banks et al. 2005)

Simulations are classified in two main categories: discrete and continuous simulations. A simulation is considered *discrete* when the state of the entities in the system change only at specific instances of time which are called *events*. Usually the term discrete-event simulation is used. A simulation is *continuous* when the state changes of entities are not discrete. This means that the continuous system state can be expressed as a continuous function. It is important to notice that simulated system can exhibit both, discrete and continuous behaviour. There can be continuously changing entities that interact with other entities at determined instances of time, which are discrete events. For example in passive radar simulation, we can assume that the targets are flying aircraft along continuous paths and radar makes observations at discrete events from these targets.

Along with discrete and continuous, simulation can be classified as *real-time* and *exhaustive* simulation. In real-time simulation, the *simulation time* is in synchronisation with the system clock maintained by the execution environment. Simulations that execute simulation time independent of system clock are considered exhaustive and execution times are desired to be as little as possible. Example use cases of real-time simulation are training systems and physics engines of video games.

3.1 Reference architecture

In simulated air surveillance training system, the purpose of simulation is to give believable impression of real systems (i.e. radars) used in air surveillance. The impression is given by simulating interactions of two categories of *entities* inside one *meta entity*. Meta entities do not interact with entities, but rather represent a boundary between simulated entities and/or system resources. The entity types used in the simulation are *targets* and *radar systems* and the meta entity is the *world*. A reference architecture for a minimal simulation system design depicting relationships between the simulated objects and world container is illustrated in Figure 4.

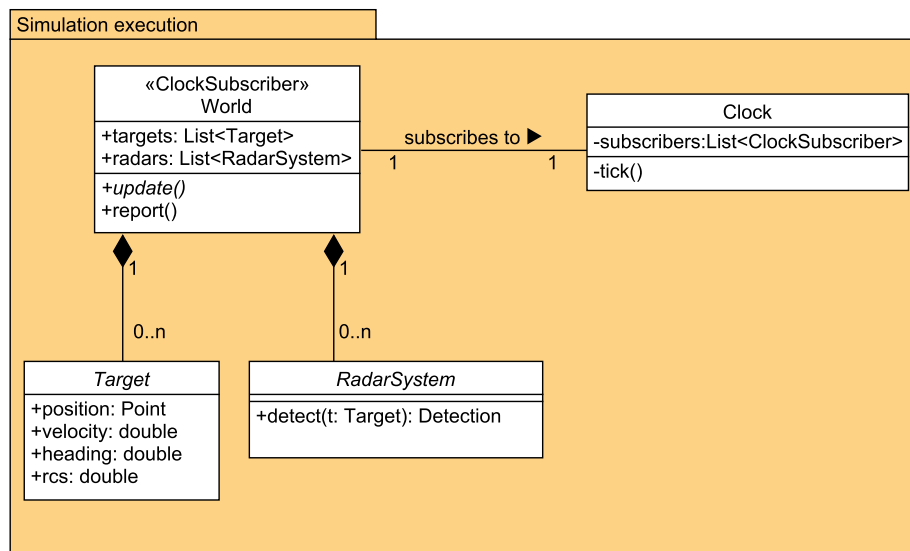


Figure 4. Simulation execution.

Targets in the simulation are given as a predefined scenario, where the state of each target is defined as a set of points in time. Points for each target describe the flight path that target takes inside the simulation or if there is only one point the target is considered stationary. The set of points can be assigned to an array and sorted for in ascending order to represent time. To read the current state of the target we assign a pointer to the index of that array. To update the current state, we increment the index once the timestamp of the point is lower than world time. Target states should provide at least information: latitude, longitude, altitude,

heading, velocity and radar cross-section.

Radar systems produce detections based on target location and other factors such as sensor location. Because there are multiple ways of configuring a radar such as varied number of sensors with different locations and attributes, they are all represented by *RadarSystem* super class. Passive radar developed in this research is considered a sub-class of the *RadarSystem* super-class and is described in chapter 5.

Scheduling in the simulation is maintained by the *Clock* by executing a *tick* function at fixed time intervals. The purpose of tick function is to run through all subscribers and call the update function to execute all scheduled events for the time period between latest and current update cycle. For the sake of simplicity, in this research we only consider case where there is one *World* instance subscribing to the *Clock*.

3.2 Target position representation

Targets and their movement are defined by set of points with location and time values. Location of the target is represented in WGS84 coordinates and altitude information. Time represented as UNIX timestamp in seconds.

Target position information is stored in an array of data points, which consist of location information in WGS84 coordinates (longitude, latitude and altitude) and time information. The array is sorted by time in ascending order, defining the path aircraft takes during the simulation, which is considered to be continuous movement.

Calculating distances on Earth's surface is more complex if the oblate spheroid geometric model is used. Assumption of spherical Earth gives 0.5% inaccuracy to latitude and 0.2% to longitude (*Admiralty Manual of Navigation* 1987). For simplicity and efficiency, the spherical model is accepted.

Distance on a sphere surface can be calculated using the law of haversines:

$$d(p_1, p_2) = 2r \arcsin \left(\sqrt{\sin^2 \left(\frac{\phi_2 - \phi_1}{2} \right) + \cos(\phi_1) \cos(\phi_2) \sin^2 \left(\frac{\gamma_1 - \gamma_2}{2} \right)} \right), \quad (3.1)$$

where ϕ_i is latitude and γ_i is longitude of point p_i , and $r = 6,378km$ is Earth's radius.

The average velocity between to points p_i and p_{i+1} is:

$$v_i = \frac{d(p_i, p_{i+1})}{t_{i+1} - t_i}, \quad (3.2)$$

where $d(p_i, p_{i+1})$ is distance. Then average acceleration between p_i and p_{i+1} can be formulated as:

$$a_i = \frac{v_{i+1} - v_i}{t_{i+1} - t_i}. \quad (3.3)$$

Acceleration cannot be determined for the last segment of the path.

For arbitrary time t , exact maneuver information is determined by interpolating the two points where $t_i \leq t < t_{i+1}$ where i represents the index in the position array.

4 Introduction to Radar

Before it is reasonable to conceptualise passive radar, we need to understand the context where the simulation model will operate: air surveillance radar systems. Radar systems are a large topic with multiple applications, so only air surveillance related applications are considered in this research. The purpose of this chapter is to give overview of radar systems in air surveillance operations and how radar operates when it is used to detect aircraft.

Radars are categorised as monostatic, bistatic or multistatic, depending on the receiver-transmitter configuration. A *monostatic* radar is a type of radar, that has a transmitter and a receiver located at the same place, and in some cases, use the same antenna for transmission and receiving. *Bistatic* radar systems take advantage of one or more transmitters in different locations than the receiver. *Multistatic* radar systems combine multiple (monostatic and bistatic) radar systems and sensors to perform data fusion and automatic tracking. (Skolnik 2001)

4.1 Basic radar operation

Radar (acronym for *RADio Detection And Ranging*) is a system, that utilises radio waves to detect flying aircraft. A basic radar system consists of four main components: transmitter, receiver, antenna and a signal processing device. The transmitter generates a signal, which is radiated by the antenna. When the signal hits an object, some of the energy is radiated from the object towards receiver. That radiated echo signal is captured by the antenna and processed by the receiver, which passes the signal for processing. Using signal processing and knowledge of the original transmission, a range (distance) to the target can be determined. In addition by analysing the Doppler shift of returned signal, the speed of the object relative to the radar can be obtained. (Skolnik 2001)(Melvin 2014)

In the event of detection, the *range* (distance) to the target is determined by measuring the time it takes for light to travel from transmitter to the receiver. Specifically range is the distance from target to receiver projected on Earth's surface. Straight line distance between the receiver and the detected target is called *slant range*.

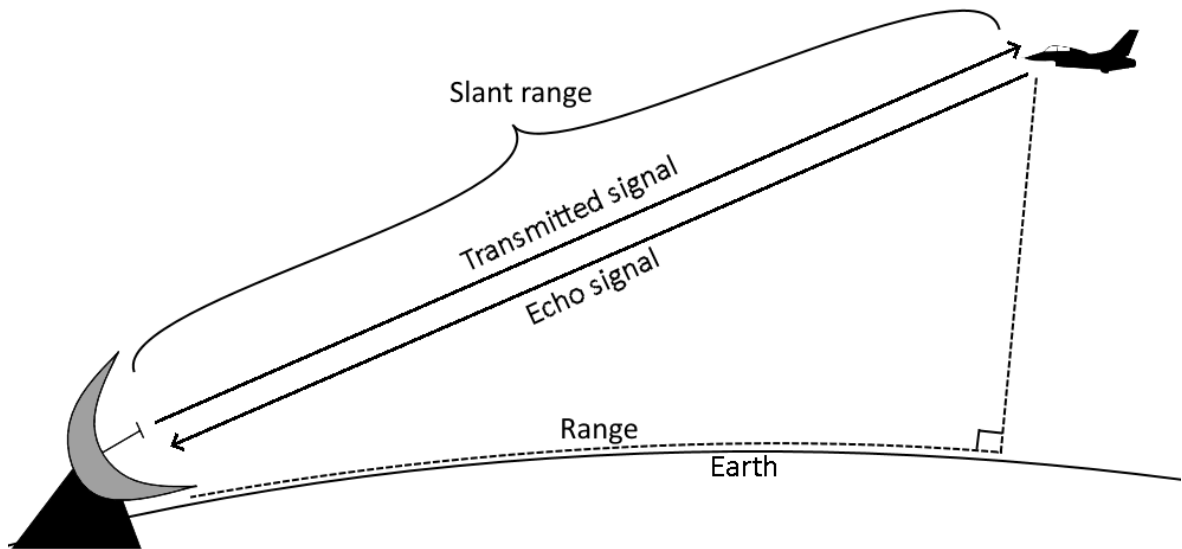


Figure 5. Basic monostatic radar.

Radar systems have to deal with constant presence of noise inside the, system which is caused by the components inside the radar and natural sources outside the system. Noise appears as random fluctuation in received signal cause disturbance in echo signal detection. Transmitted signal is several orders of magnitude stronger than the echo signal due to fast decline in signal power over distance. *Detection threshold* is used to describe the minimum signal strength required for an echo signal to yield a detection. Signal strength is heavily affected by distance travelled, hence detection threshold essentially defines the maximum detection range of the radar. By lowering detection threshold, even weaker signals would yield detections at a cost of higher chance of *false detections*, which are caused by random signals picked from the noise. Background noise can be suppressed with various methods due to its random nature.(Skolnik 2001)

Figure 6 demonstrates an example case, where output of a processed incoming signal in time. There are three peaks among the noise that represent real target echoes, and due to high threshold for detection, the detection number 2 is missed. On the other hand, low detection threshold increases risk of false detections.

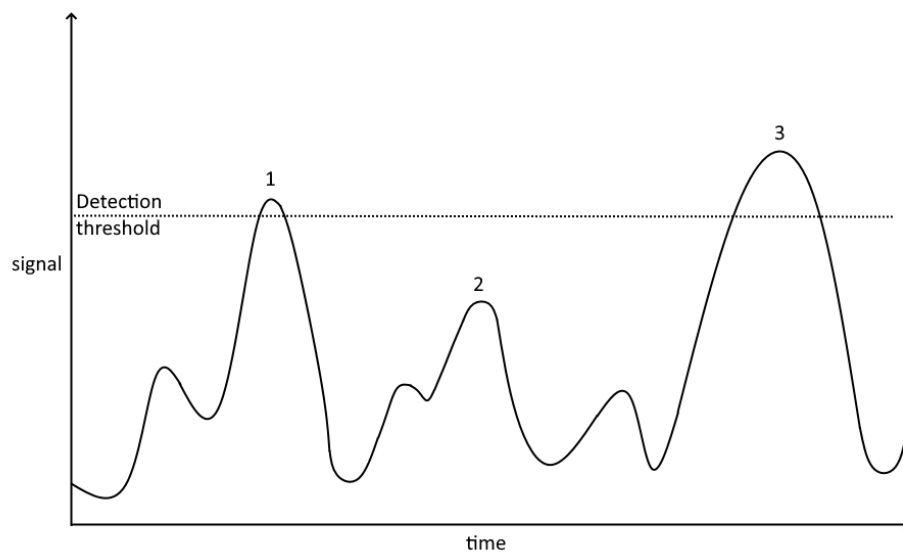


Figure 6. Detection threshold example.

Detections caused by *clutter* are detections of objects that are real (not from noise or interference), but not interesting to the particular radar application. Clutter can be filtered out by examining the nature of similar detections for long periods of time. For example in air surveillance, clutter caused by mountain or building is very static in nature and can be filtered out. (Skolnik 2001)

Jamming is referred intentional or unintentional disturbance of a radar by transmitting signal towards the radar in its operational frequency (Skolnik 2001). In electronic warfare, jamming is a common method used to mask targets.

Radar systems use electromagnetic radiation with frequencies ranging from 3 kHz to 300 GHz, which are essentially the radio frequency range (3 kHz to 300 MHz), and the microwave frequency range (300 MHz to 300 GHz) (R. Timothy Hitchcock 2004). Since the second World War, the radar frequency bands were designated by letters to describe uses of different subset of radio frequencies and their uses. Today there are many different radio frequency band designations to describe the frequency range a particular radar operates at: IEEE Standard Radar Nomenclature (521-1984 1984), International Telecommunications

Union (ITU) Radar Band Nomenclature, Military Radar Band Designations. Table 1 lists the IEEE standard 521 frequency bands.

Different frequencies produce different wavelength of radio signals, which in turn affect the performance of the radar (Skolnik 2001). Band designations are used as a quick reference to characteristics of the radar. The right most column in the Table 1 are defined in the results of the World Administrative Radio Conference of 1979. (521-1984 1984).

Band designation	Nominal Frequency Range	Specific Frequency Ranges for Radar Based on ITU Assignments for Region 2
HF	3 MHz - 30 MHz	
VHF	30 MHz - 300 MHz	138 MHz–300 MHz 216 MHz–225 MHz
UHF	300 MHz - 1000 MHz	420 MHz–450 MHz 890 MHz–942 MHz
L	1 GHz - 2 GHz	1215 MHz–1400 MHz
S	2 GHz - 4 GHz	2300 MHz–2500 MHz 2700 MHz–3700 MHz
C	4 GHz - 8 GHz	5250 MHz–5925 MHz
X	8 GHz - 12 GHz	8500 MHz–10,680 MHz
K_u	12 GHz - 18 GHz	13.4 GHz–14.0 GHz 15.7 GHz–17.7 GHz
K	18 GHz - 27 GHz	24.05 GHz–24.25 GHz
K_a	27 GHz - 40 GHz	33.4 GHz–36.0 GHz
V	40 GHz - 75 GHz	59 GHz–64 GHz
W	75 GHz - 110 GHz	76 GHz–81 GHz 92 GHz–100 GHz 126 GHz–142 GHz
mm	110 GHz - 300 GHz	144 GHz–149 GHz 231 GHz–235 GHz 238 GHz–248 GHz

Table 1. IEEE Std 521-1984 Radar frequency band nomenclature.

4.2 Passive bistatic radar

Compared to monostatic radar, a *passive bistatic radar* utilises non co-operative radio transmissions such as TV and radio stations as transmitters, called *illuminators*. Passive radar

has at least two receivers; one for *surveillance channel* and one for *reference channel*. The reference channel listens for one or more incoming transmissions and surveillance channel for echo signals. The samples from surveillance channel are matched with samples from reference channel, and if the sample contains a piece of the original transmission, a detection is found. Passive radar can also be called passive bistatic radar (hence being bistatic radar by definition), passive coherent location (PCL), piggy-pack radar, passive covert radar, parasitic radar, opportunistic radar and broadcast radar (Melvin 2014).

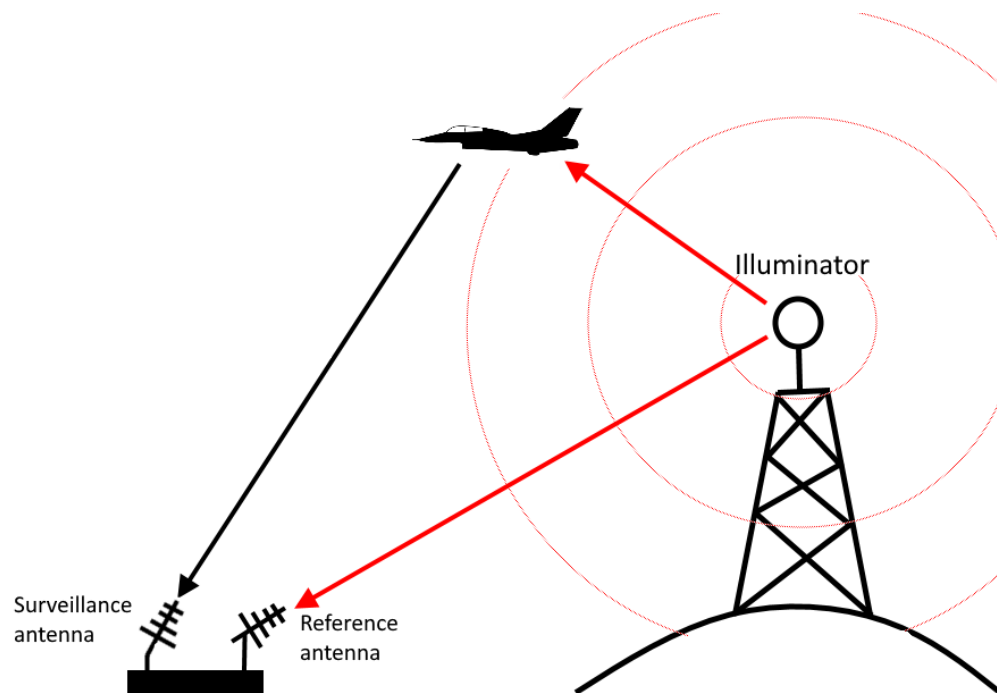


Figure 7. Simple passive radar example.

Passive radar is distinct from other bistatic and multistatic radars by two main features. Passive radar use non-cooperative transmitters which are not controlled by the operator of the passive radar. Secondly, the broadcast used is only a portion of the possible signal frequency spectrum that can be used.

Detection with passive radar happens by matching the signal from surveillance channel to the signal of reference channel, typically with using matched filtering. Mathematically, the range to the target is determined by the signal travel time from transmitter to target and from target to the receiver. The path signal takes in the detection scenario has a length of $(R_t + R_r)$,

where R_t is distance from transmitter to target and R_r is distance from target to receiver. Points that can produce a path of this particular length form an ellipse with transmitter and receiver being the two focal points separated by distance L . (Melvin 2014)

There are different methods to extract target position from detection information . Depending of the antenna configuration, if azimuth α to the target from receiver is known, the location can be calculated using equation (Melvin 2014):

$$R_r = \frac{(R_t + R_r)^2 - L^2}{2(R_t + R_r + L \sin \alpha)}, \quad (4.1)$$

where $(R_t + R_r)$ is known to be the signal path transmitter-target-receiver, demonstrated in Figure 8. If three or more transmitters are used, triangulation using the multiple ellipses formed by receiver-illuminator pairs, demonstrated in Figure 9 (Melvin 2014). When two illuminators are used, a special method like digital beamforming have to be utilised in order to achieve target location (Malanowski and Kulpa 2008).

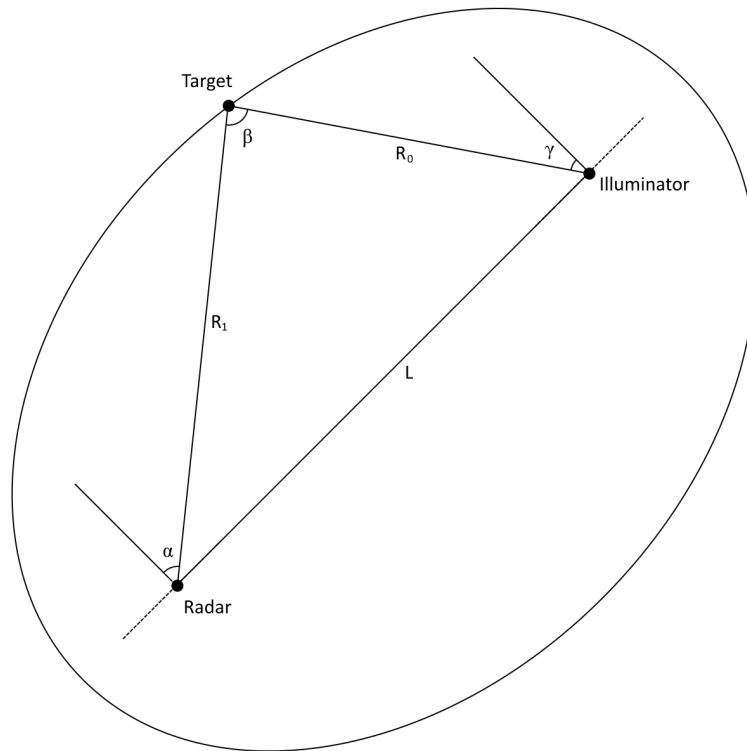


Figure 8. Target position in bistatic detection.

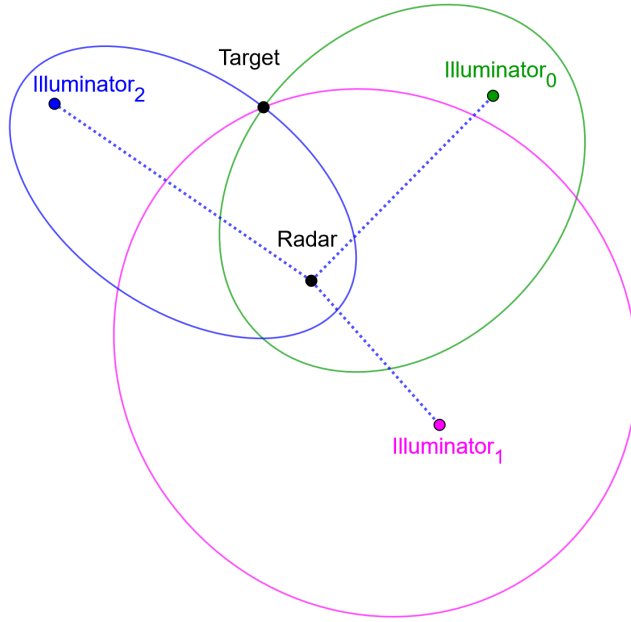


Figure 9. Target location with triangulation.

For any radar system, the performance analysis begins with understanding the *radar equation*. A radar equation is a mathematical tool, that can be used to assess detection performance of a radar in given circumstances. In passive bistatic radar analysis the basic form of bistatic radar equation is used to calculate *signal-to-noise ratio* (SNR) (H. Griffiths and C. Baker 2005):

$$\frac{P_r}{P_n} = \frac{P_t G_t}{4\pi R_t^2} \cdot \frac{\sigma_b}{4\pi R_r^2} \cdot \frac{G_r \lambda^2}{4\pi} \cdot \frac{1}{kT_o BF} \cdot L \quad (4.2)$$

where

P_r is the received signal power,

P_n is the receiver noise power,

P_t is the transmit power,

G_t is the transmitting antenna gain,

R_t is transmitter-to-target range,

σ_b is the bistatic radar cross-section,

R_r is the target-to-receiver range,

G_r is the receiver antenna gain,

λ is the signal wavelength,
 k is Boltzmann's constant,
 T_0 is the noise reference temperature of 290 Kelvin,
 B is the receiver effective bandwidth,
 F is the receiver noise figure and
 L are general system losses.

Signal-to-noise ratio is an important value in radar performance analysis. SNR essentially describes how much there is "real" signal received from a target in proportion to how much noise is in the receiver system. In the radar equation 4.2 the thermal noise power is represented by

$$P_n = \frac{1}{kT_0BF} \quad (4.3)$$

and receiver signal power by

$$P_r = \frac{P_t G_t G_r \lambda^2 \sigma_b}{(4\pi)^3 R_t^2 R_r^2}. \quad (4.4)$$

Typically, SNR and other signal processing parameters are represented with decibels:

$$\left(\frac{P_r}{P_n}\right)_{dBm} = 10 \log_{10}\left(\frac{P_r}{P_n}\right) = 10 \log_{10}(P_r) - 10 \log_{10}(P_n). \quad (4.5)$$

As it was stated before, in order to detect a target signal strength must surpass the detection threshold. For SNR, the same concept applies: the higher the SNR, the higher the probability of detection.

The signal is not only transmitted over the carrier frequency, but rather is spread at sides in spectrum wide as the bandwidth. To increase sensitivity of the receiver, and also SNR, radar systems can use coherent (or noncoherent) integration. This integration/processing gain is determined by the measurement period called the maximum integration time T_{max} and the effective bandwidth of the signal B :

$$G_p = T_{max}B. \quad (4.6)$$

The effective integration time is limited by the maneuver of the target and signal characteristics, and the effects can be approximated with equation (H. D. Griffiths and C. J. Baker 2017):

$$T_{max} = \left(\frac{\lambda}{a_r}\right)^{(1/2)}, \quad (4.7)$$

where a_r is radial component of target's acceleration and λ is wavelength. This effect is caused by Doppler and range cell migration, which happens if target moves radially towards the illuminator or the receiver. Other restricting factor to maximum effective integration time is how long target echoes are coherent during the integration. Processing gain is significant factor for passive radar performance, especially in DVB-T and FM types (H. D. Griffiths and C. J. Baker 2017).

Radar cross-section (RCS) is used to describe object's size in terms of reflecting surface area and it is defined in square meters. RCS depends on the detectable object size as well as the material object is made of and orientation respective to the radar (Skolnik 2001). For bistatic radar systems, RCS is usually considered higher than monostatic equivalent. With regards to stealth aircraft, which are designed to have small RCS by scattering incoming radio signals from monostatic radars to different directions, are more easily detected by bistatic passive radars (H. D. Griffiths and C. J. Baker 2017).

In real world, the measured RCS of an aircraft is not constant due to complex shape of the reflecting surface, which causes fluctuation in the real RCS (Skolnik 2001). Fluctuations of targets and its effects on radar performance were modeled by Peter Swerling (Swerling 1954) categorised into four types (today called Swerling type 1, 2, 3 and 4). Swerling target fluctuation models are used to predict probability of detection in radar systems and is applicable to be used with passive radars as well (Pölönen and Koivunen 2013).

Because passive radars operate with non-cooperative transmitters and cannot interact when to transmit signal and illumination sources are omnidirectional in nature, receivers are constantly required to deal with direct signal interference (DSI). Amount of DSI depends in direct signal strength

$$P_d = \frac{P_t G_t G_r \lambda^2}{(4\pi)^2 L^2}. \quad (4.8)$$

Signal-to-interference ratio (SIR) is defined as ratio of received echo signal P_r and direct line of sight (LOS) signal P_d across the baseline.

$$P_{sir} = \frac{P_r}{P_d}. \quad (4.9)$$

SIR effects on performance is determined by the dynamic range of the analog-to-digital converter (ADC) used in the radar system. Unlike noise's effects to SNR, effects of DSI

to SIR cannot be reduced using integration since the direct signal is amplified by the same principle as echo signal. In order for the signal to be detectable under effects of DSI, the SIR p_{sir} must be larger than reciprocal of the dynamic range of the ADC:

$$P_{sir} > \frac{1}{ADC_{DR}}. \quad (4.10)$$

(Melvin 2014) (Brown 2013)

Strong interference from direct signal is a common problem in passive radars and multiple methods exist to achieve better SIR: physical shielding, fourier processing, high-gain antennas, sidelobe cancellation, adaptive beamforming and adaptive filtering (Melvin 2014).

4.3 Antenna properties

In radar system, antenna is responsible for transmitting and receiving radiated and reflected signals and as it was previously observed from radar equation, antenna gain plays key role in received signal strength. Antenna gain represents the amount amplification or reduction the antenna provides to received or transmitted signal. The amount of gain the antenna provides in various situations is defined by its orientation and *radiation pattern*. Radiation pattern describes antenna's sensitivity or directivity as a function of horizontal axis (azimuth) and vertical axis (elevation).

Radiation pattern is typically graphed into two tables one depicting horizontal and second vertical angles, which then together form a three dimensional representation. Figure 10 demonstrates radiation pattern of a half-wave dipole antenna, which has omnidirectional radiation in horizontal axis and a figure eight like shape in vertical axis. In three dimensions, the pattern has a doughnut like shape Figure 11 (created by:(Yannopoulou and Zimourtopoulos 2011)). The hypothetical isotropic antenna radiates uniformly in all directions, and therefore its radiation pattern resembles a perfect sphere.

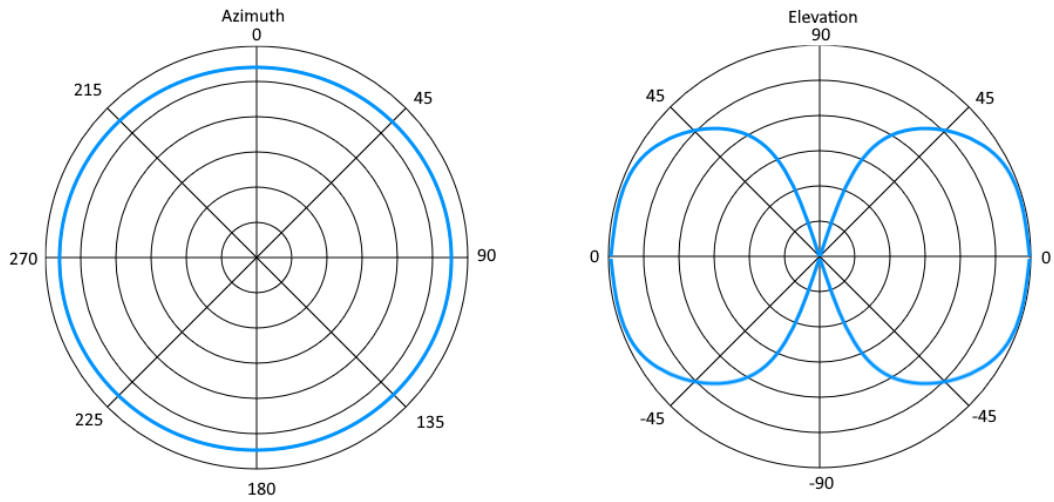


Figure 10. Radiation pattern of half-wave dipole antenna in 2D

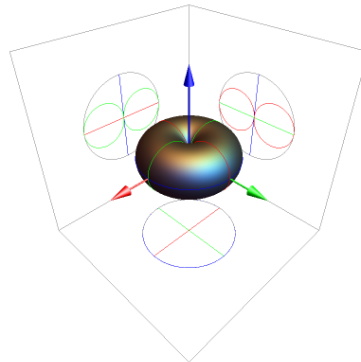


Figure 11. Radiation pattern of half-wave dipole antenna in 3D.

Radiation pattern consists of three types of lobes: main lobe, side lobe and back lobe. Main lobe is the part, where the gain is at its highest peak and side lobes are minor, weaker sections of the pattern. Back lobe is in opposite direction of the main lobe. Parts where graph collapses to the origin, are called nulls. The best antenna for radar is a radar with strong main lobe and very weak side and back lobes (Skolnik 2001).

Radar antennas are usually constructed in such a way that it has high directivity and narrow beam. The *beamwidth* (or half-power beamwidth) is the angle between points where antenna

gain is 3 db lower than the main lobe peak gain. Antenna types used in passive radars (presented in section 4.4) include parabolic, dipole, yagi and horn antennas.

4.4 Passive radar demonstrations in research

This section covers historical and modern demonstrators of various passive radars. For the model conceptualisation, it was decided that following key attributes were paid special interest to: transmitted signal characteristics (transmit power, carrier frequency and bandwidth), type and properties of antenna configuration used for surveillance and reference channels, typical detection range and overview of the operation and composition. Comprehensive examination of the signal processing scheme was left out as out of scope.

Historical passive radar concepts

The concept of passive radar is dated to the very first radar demonstrations in the history of radar. In February 1935, Watson Watt and Wilkins conducted the first recorded air surveillance radar experiment also known as the Daventry Experiment, in which they were able to detect a bomber aircraft from 8 miles using BBC Empire transmitter with frequency of 6.1 MHz and 10 kW power. This led to the future development and deployment of the early warning system of Britain: Chain Home. (Melvin 2014)

The first recorded "truly parasitic" passive radar was the German developed radar system by the name Klein Heidelberg (KH) during the Second World War (Griffiths and Willis 2010). KH used the British Chain Home (CH) transmitters as its illumination source and reports state that it could detect aircraft up to 300-400 km. CH transmitters operated at high peak power of 250 kW and 750 kW later in the war with 20 microsecond pulse duration and low pulse repetition frequency of 12.5 Hz or 25 Hz. The transmission of CH had very broad beam width, which was suitable for KH receivers to use. The antenna consisted of array of 18 half wavelength dipole antennas divided in 6 groups, each set having 3 adjacent antennas and beamwidth was approximately 45°. KH typically was used to scan a 100° sector and reports suggest that while the antenna array could be rotated to cover a full 360° revolution, it was denied from operators to avoid damaging the cable connections. Direct signal to reference channel was captured using horizontal dipole antenna 60 meters away from KH surveillance

antenna.(Griffiths and Willis 2010)

Tracking and target positioning with KH, was done by taking multiple measurements of the target after it was initially picked up. After the initial observation was made, operator would turn the antenna towards the target to achieve maximum signal strength to get bearing and range sum. Total of 40 measurements were taken after passing the information on to command and control. (Griffiths and Willis 2010)

After the war, the USA developed Sugar Tree system, which was an over-the-horizon system that was deployed to detect possible USSR ballistic missile launches. The system utilised short-wave radio broadcasts as illuminators. (Melvin 2014)

FM radio based passive radars

University College London introduces a passive radar utilising FM radio based illuminator at 98.5 MHz frequency. Antenna used for both surveillance and reference channels, was a 4 element yagi antenna with 8 dBi gain and 105° half power beamwidth. This experimental radar achieved a measured detection from range of at least 92 km. (O'Hagan et al. 2007)

In Warsaw University of Technology (Malanowski, Kulpa, and Misiurewicz 2008), researchers constructed a total of three passive radar demonstrators PaRaDe-1, PaRaDe-2 and PaRaDe-C. Radars 1 and 2 were stationary systems installed on university building and PaRaDe-C was a installed on a car. PaRaDe-2 and PaRaDe-C antenna array consisted of eight half-wave dipole antennas arranged in a circular pattern, one of these being the reference channel, thus forming a 330° wide beam for surveillance channel with . Digital beamforming was used to divide surveillance channel into seven beams, allowing direction of arrival (DOA) estimations (Malanowski and Kulpa 2008). The best recorded results with PaRaDe were a detection of a target with approximately $10 m^2$ RCS from monostatic equivalent range of 370 km with illuminator having high power of 60kW transmission (Malanowski et al. 2012).

Researchers at School of Electronic Information of Wuhan (Xie et al. 2018) demonstrated a multiple illuminator FM radio based software defined passive radar. Surveillance and reference antenna setup was similar to the mentioned PaRaDe setup (Malanowski and Kulpa 2008), sampling was done digitally with FPGA devices and stored on PC to perform pro-

cessing, detection and tracking. Reference signal was captured from beams produced by digital beamforming using the surveillance antenna beams that were pointing towards the transmission tower. Results showed that detection accuracy is heavily influenced by the type of program broadcasted on the radio, music having a stable bandwidth and speech having lots of variation. Combining multiple transmission sources improves detection accuracy greatly. Transmission stations had 3 kW power transmission and were located 14.1 km and 37.7 km away from the test site. Detection ranges up to 60 km were achieved with altitudes lower than 5 km when detecting planes landing on nearby airport.

Analog television based radar

At DERA Malvern (P.E.Howland 2008) television broadcast illumination based passive radar and tracker was demonstrated. The radar used the TV vision and sound carrier signals to detect targets. Experiment radar used transmitter located at Crystal Palace and radar was at Pershore. Antenna configuration consisted of two yagi-uda antennas set 0.6 wavelength apart allowing DOA estimation and 112° beamwidth. Radar system performed target tracking with Doppler and DOA measurements using Kalman filter.

Digital television based radars

Australia Government's Department of Defence (Palmer et al. 2009) published a report with experimental results of DTV-T illuminator based passive radar. Antenna configuration for surveillance channel consisted of 15 element yagi antenna with 13 dB gain. Digital television transmission of carrier frequency 564.5 MHz was used and the bandwidth with a true bandwidth of 7.5 MHz. As result, detection of vehicles on road at range of 1200 meters and aircraft at range of 10 kilometers with CFAR detection. Processing gain of the system was 3.24 dB and minimum SNR for detections 13 dB.

Researchers at Budapest University of Technology and Economics (Pető et al. 2014) experimented DVB-T illuminator based software defined passive radar to detect airplanes. Antenna configuration of the surveillance channel consisted of a yagi antenna with 15 dB gain. Carrier frequency of the signal used was 610 MHz. The USRP software defined radio device captured the signals which were transferred to a PC via Ethernet. Labview program per-

formed the calculations from the data and displayed results. Experiment results showed a successful detection at 2.3 km range and the broadcast station was transmitting with 100 kW power.

St. Petersburg Electrotechnical University (Vorobev et al. 2018) researchers built a passive radar with DVB-T2 illuminator. The system was capable of detect and track moving targets and estimate range, velocity and exact position and draw them on a map. Antenna configuration of surveillance channel consisted of 14 element phased antenna array (original design had 16 elements (Vorobev, Barkhatov, and Kutuzov 2017)) with maximum gain of 24 dB. Digital beam forming was used to separately process each antenna array element to get azimuth of target detections (Vorobev, Barkhatov, and Kutuzov 2017). Results of experiments report detection ranges of various types of aerial targets from small targets such as an UAV ($0.01 m^2$), to a passenger aircraft ($15 m^2$) with detection ranges from 13.9 km to 86 km respectively with illuminator operation at 5 kW peak power (Barkhatov, Vorobev, and Konovalov 2017).

A recently published demonstration VHF DVB-T signal based passive radar from Warsaw University of Technology (Płotka et al. 2020). Radar consisted of multiple analog front-ends for signal gathering with total of five for surveillance and one for reference signal. Antenna configuration consisted of 4 element uda-yagi antennas with gain from 6 dBi to 8 dBi and operating frequencies from 170 MHz to 230 MHz. Two experiments were conducted: first in a forest and second in an open field and a target was a Cessna plane. In forest experiment a maximum of 10 km detection range was recorded and open field scenario resulted in 15 km range, illuminator was broadcasting at 10.4 kW power.

GSM based passive radars

At Nanyang Technological University (Sun, Tan, and Lu 2008), a passive radar demonstrator using GSM signals as illuminators of opportunity was constructed. Antenna configuration for surveillance channel consisted of four horn antennas pointed at same horizontal and vertical direction with physical spacing of 0.255 meters (corresponding to 0.8 wavelength) each having 5.5 dB gain and 60° beamwidth at 940 MHz. GSM base station was located 1032 meters from the test site and operated at less than 50 Watts. For the test, a carrier frequency

of 940.2 MHz was chosen. Results showed that an airliner was detected at range of 4 km.

UMTS based software defined radars

Researchers at University of Pisa (Petri et al. 2010) experimented with a software defined passive radar utilising UMTS illuminator. This radar used parabolic antennas which were optimised for frequency range of 2.12-2.35 GHz. Both, the reference and the surveillance channel used this antenna. Both surveillance and reference channel antennae had gain of 22.5 dBi and 10° half power beam width. In the demonstrator experiment, a moving truck was detected at range of 240 meters.

Researchers at Ankara University (Satar et al. 2018) published a paper of a "do it yourself" passive radar from COTS components based on UMTS illumination. Signal types used for the experiment were GSM signals and the equipment was capable of using LTE signals too. Antennas used in reference and surveillance channel were parabolic antennas with 9° beamwidth. Detection ranges varied from 200 to 240 meters implying short range surveillance capability. System composition consisted of two antennas connected to a RF module that digitises the data from surveillance and reference channel to FPGA card module that pre-processes the data for processing system implemented with MATLAB.

WiMAX based passive radar

Nanyang Technological University of Singapore evaluated, that a WiMAX illuminator based passive bistatic radar is capable of detecting moving ships near shore, moving bus on a road and running people on the street. The antenna configuration was a horn antenna tuned to 2.38 GHz, had 11.97 dBi gain and 60° beamwidth. Results showed detection ranges around 450-750 m for larger object like buses and ships, and 200 m for human body. This radar experiment processed detections offline from the recorded signal data of the two channels. Authors suggest that improved signal processing and faster equipment could make real time surveillance possible. (Qing Wang and Lu 2010).

4.5 Illuminator

The non-cooperative radio transmitter in passive radar context is called an *illuminator*. From passive radar examples mentioned in section 4.4, possible illuminators for passive radar are radio, analogue and digital TV, GSM and UMTS communication, GPS satellites, WiFi and WiMAX communication. Important attributes of illuminators are its typical carrier frequency used, bandwidth of modulated signal, effective radiated power (ERP) and radiation pattern of the antenna (Brown 2013).

In general, digital signal performs better in radar applications compared to analog signal because analog signal is dependent on the broadcast content which affects the performance. Digital signals are more noise like and the whole bandwidth is more filled with information than analog signal.(H. D. Griffiths and C. J. Baker 2017) Digital technologies include for example GSM (Global system for Mobile communications), G3/4, DAB (Digital Audio Broadcast), DRM (Digital Radio Mondiale), DVB-T (Digital Video Broadcast-Terrestrial), WiFi and WiMAX.

FM Radio broadcasting is frequency modulated (FM) analogue radio transmission for audio, like music or speech. Radio frequencies span, depending on region, around the VHF band from 88 MHz to 108 MHz and effective radiated power can be as high as 250 kW and bandwidth of the modulated signal is typically 50 kHz. Range and doppler resolution of VHF FM radio is relatively poor and is dependent on the broadcast content. With proper techniques such as using adjacent channels from same transmitter can improve accuracy. (H. D. Griffiths and C. J. Baker 2017)

Analogue TV is old technology and is being replaced with digital television, however some demonstrations have been developed to analogue TV. Analogue TV transmission is around UHF band from 500-600 MHz with high 1 MW power and 5.5 MHz bandwidth. Range resolution with analogue TV is around 30 m with these parameters.(Melvin 2014)

Digital radio technologies include Digital Radio Mondiale (DRM) and Digital Audio Broadcast (DAB). DRM is not widely used by many countries and several have abandoned the transition to move from FM audio broadcasts to DRM. DRM proves to be good source of illumination from short range surveillance with passive radars (maximum 16 km range). DAB

transmissions have a typical frequency around 220 MHz with 220 kHz bandwidth and 10 kW transmission power. (H. D. Griffiths and C. J. Baker 2017)

Digital television broadcasts transmit video and audio transmissions in digital format. DVB-T is commonly used in today's passive radars for medium range surveillance. Typical transmission power can vary from 2 kW up to 8 kW and effective bandwidth of 6-8 MHz provides good resolution in doppler and range. (H. D. Griffiths and C. J. Baker 2017) Carrier frequency depends on country and region. For example, in Finland channel carrier frequencies span from 482 MHz to 706 MHz (Digita 2020).

GSM is a standard developed by European Telecommunication Standard Institute (ETSI) for second generation cellphone networks. Carrier frequency ranges are spanned from 900 MHz to 1.8 GHz and effective bandwidth is 150 kHz which provides approximately 1 km range resolution. Typical GSM base station operates at 100 W power which provides short ranges. Given these properties, GSM is not well suited for accurately detect and track aircraft. (H. D. Griffiths and C. J. Baker 2017)

Long-Term Evolution (LTE) waveform is used with 3G and 4G signals transmitted with OFDM subcarriers. LTE carrier frequencies are spread across 729 MHz to 3.8 GHz and channels are divided to 72 to 1320 subcarriers with bandwidth varying from 1.4 MHz to 20 MHz. Effective bandwidth for passive radar use of LTE illuminator would be approximately 5 MHz (H. D. Griffiths and C. J. Baker 2017) and transmission power varies from 50 to 100 W. LTE provides good range and doppler resolution for short range surveillance.

Wifi and WiMAX signals is suitable for short range high resolution surveillance with under 100 m range. For small drone surveillance WiFi or WiMAX would provide adequate source of illumination when used in multistatic configuration.

There are generally two major types of satellite illuminators: geostationary such as GNSS, GPS, INMARSAT, GLONASS, GALILEO and BeiDou, and non geostationary such as Low Earth Orbit Remote-Sensing Satellites and IRIDIUM (H. D. Griffiths and C. J. Baker 2017). Geostationary satellites provide continuous illumination which enable integration gain but suffer from very low power density at Earth's surface (H. D. Griffiths and C. J. Baker 2017). Non geostationary satellites have higher power density on surface but provide very short illu-

mination time (H. D. Griffiths and C. J. Baker 2017).

5 Passive radar model conceptualisation

5.1 Passive radar components

Section 4.4 describes different passive radar demonstrations. Based on the radar demonstrators, an abstract architecture of passive radar system components was created. Overview of the passive radar concept architecture is illustrated in Figure 12 (UML).

The passive radar system is a composition of one or more passive bistatic receivers which enable multistatic configuration. Radar system is assigned to a Target which provides the position information. The *rotating* boolean value is used to control if the surveillance channel antenna arrays should be rotating or stay statically in place.

Passive bistatic pair is considered to form a bistatic pair with associated illuminator, that is a target with Illuminator instance attached to it. Target information is required to get position of the illuminator. Most of the passive radar demonstrations are composed of one such pairs, but literature suggests that multiple receiver-illuminator would be ideal for a passive radar to locate targets with triangulation. This approach makes design of multistatic passive radar simulation design possible. Bandwidth, dynamic range, detection threshold, digital beamforming, direction finding and physical shielding affect the simulated signal processing which is described in section 5.5.

Antenna parameters are defined in the AntennaConfiguration class that is used in simulated signal processing. Reference and surveillance channels consist of antennas that feed into them. Reference antenna is always pointing to the illuminator and therefore some of antenna configuration values are direct signal strength is affected by distance only. Surveillance channel's antenna array can be constructed from multiple antennas and each antenna forming the surveillance channel coverage is configured separately. section 5.2 explains how the GainTable is used when defining gain of the antenna in signal processing scenarios.

Illuminator class acts as a wrapper for illuminator parameters and is attached to a target which allows simulated signal processing take advantage of the target location for calculations. ERP stands for *effective radiated power* and is the output power in Watts of the

illuminator. Antenna configuration and its radiation pattern is used in both direct signal and echo signal calculation, described in section 5.5.

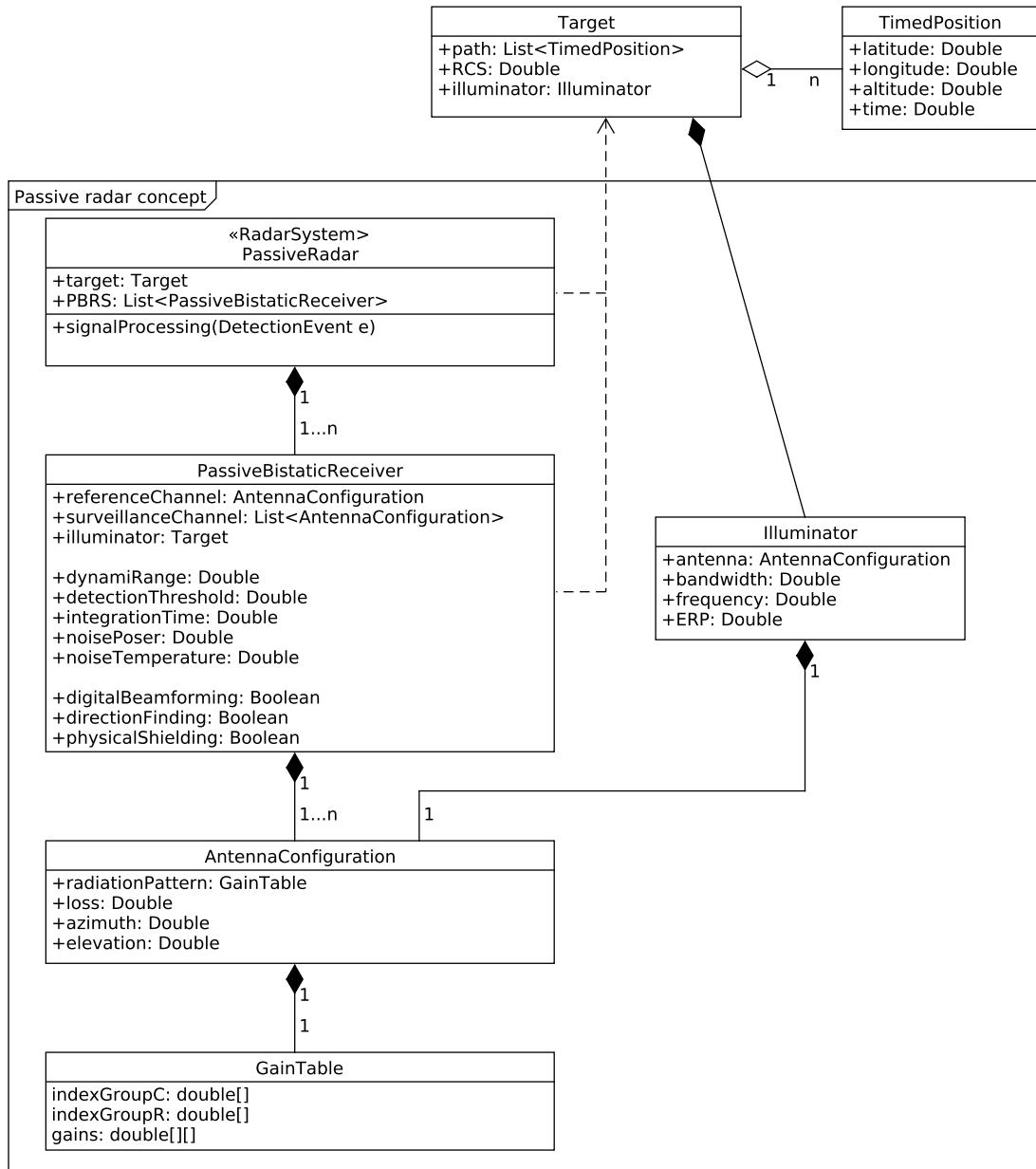


Figure 12. Passive radar model architecture overview in UML

Figure 13 demonstrates the relationship between the conceptualised architecture and typical passive radar components presented in (Melvin 2014) and (O’Hagan et al. 2007). Antenna configuration describes antenna parameters that affect the gain they provide in processing

and losses. Passive bistatic receiver has most of the functionality performing the simulated processing of the signal. Passive radar class could be also depicted as a wrapper class for all the functionality.

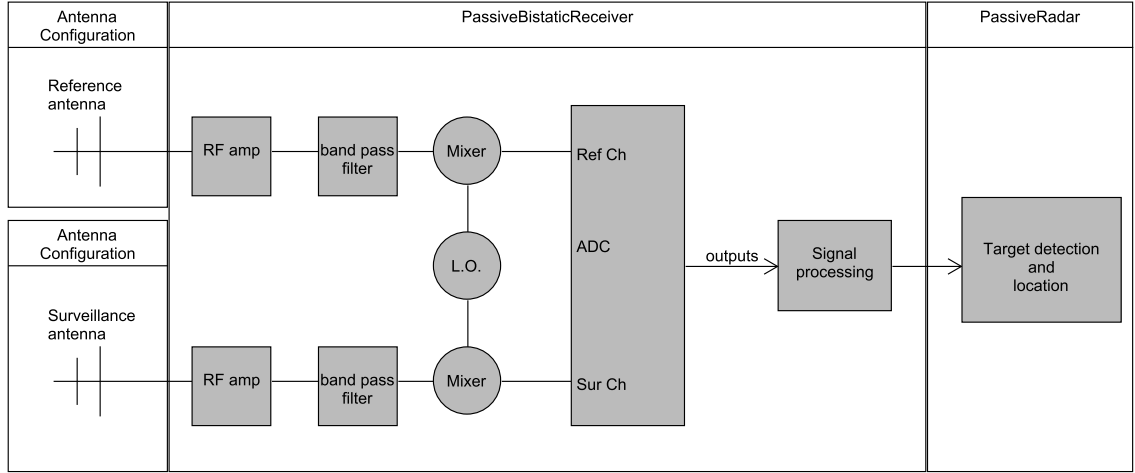


Figure 13. Passive radar components and their relation to model

5.2 Antenna gain

Radiation pattern describes gain provided by the antenna when target's relative azimuth and elevation to the antenna are known. Pre-calculating and configuring antenna pattern into a $N \times M$ gain table where corresponding azimuth values are arranged in columns and elevation values in rows. Gain table index group for columns (I_C) is formed from selected azimuth values in ascending order:

$$I_C = \{n \in \{0, \dots, N\} \mid \alpha_n \in [0, 2\pi], \alpha_n < \alpha_{n+1}, \forall n < N - 1, \alpha_0 = 0, \alpha_n = 2\pi\}$$

and similarly for row index group (I_R) from elevation values:

$$I_R = \{m \in \{0, \dots, M\} \mid \varepsilon_m \in [-\pi/2, \pi/2], \varepsilon_m < \varepsilon_{m+1}, \forall m < M - 1, \varepsilon_0 = -\pi/2, \varepsilon_m = \pi/2\},$$

demonstrated in Table 2.

	$\alpha_0 = 0$	α_1	\dots	$\alpha_n = 2\pi$
$\varepsilon_0 = -\pi/2$	G_{00}	G_{01}	\dots	G_{0n}
ε_1	G_{10}	G_{11}	\dots	G_{1n}
\vdots	\vdots	\vdots	\ddots	\vdots
$\varepsilon_m = \pi/2$	G_{m0}	G_{m1}	\dots	G_{mn}

Table 2. Gain table demonstration.

Gain table values G_{ij} have following constraints:

1. $G_{0i} = a$ and $G_{mi} = b \forall i \in I_R$
2. $G_{j0} = G_{jn} \forall j \in I_C$

Gain table values form a reference values for antenna gain in all directions. Bilinear interpolation is applied to approximate values between points smoothly and with constraints 1 and 2, the surface is continuous. Constraint 1 ensures that when approaching the poles gain values converge to same point. Constraint 2 ensures that when approaching 2π or 0 from either side, the path along meridian is continuous. From Figure 14, a geometric demonstration of the transformation of the elevation and azimuth value mesh into sphere surface.

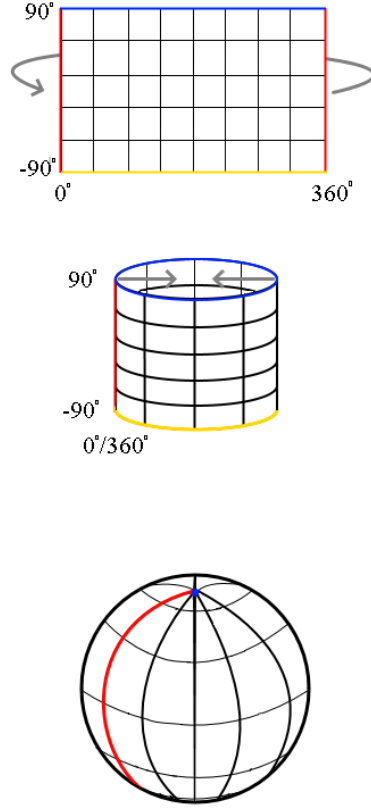


Figure 14. Gain table mesh into sphere transform.

Antenna gain is determined by function:

$$\begin{aligned}
 F_g : [0, 2\pi] \times \left[\frac{-\pi}{2}, \frac{\pi}{2} \right] &\longrightarrow \mathbf{R}, \\
 F_g(\alpha, \varepsilon) &= \frac{1}{(\alpha_{j+1} - \alpha_j)(\varepsilon_{i+1} - \varepsilon_i)} \\
 & (G_{ij}(\alpha_{j+1} - \alpha)(\varepsilon_{i+1} - \varepsilon)) + \\
 & G_{(i+1)j}(\alpha - \alpha_j)(\varepsilon_{i+1} - \varepsilon) + \\
 & G_{i(j+1)}(\alpha_{j+1} - \alpha)(\varepsilon - \varepsilon_i) + \\
 & G_{(i+1)(j+1)}(\alpha - \alpha_j)(\varepsilon - \varepsilon_i)),
 \end{aligned} \tag{5.1}$$

where G_{ij} corresponds to gain table values resolved by relative azimuth $\alpha_j \leq \alpha < \alpha_{j+1}$ and elevation $\varepsilon_i \leq \varepsilon < \varepsilon_{i+1}$ from respective index groups I_C and I_R .

5.3 Execution overview

Simulation program aggregates preliminary detection candidates from all targets in the scenario. Each detection candidate is then processed by the simulated signal processing, which determines if the target is detected by the radar, see section 5.5. If a detection is decided to be made, a plot is created and given into the training system for tracking and operators to inspect. The data aggregation is configurable and in this research a 2 second period was used.

5.4 Pre-processing detection candidates

In the simulation, the position of both receiver and illuminator is expected to be known. There are essentially two major limiting conditions for detection candidate to produce a real detection (a plot in our case). First, the target must be in receiver's and illuminator's *line of sight*: they are not hidden behind the horizon that would almost completely absorb any signal. Second, the signal processing should produce high enough SNR for detection, discussed in section 5.5.

Two entities are visible above their respective horizons if the combined distance between the entities is less than combined distance to their horizons. Earth is considered an oblate spheroid rather than perfect featureless sphere and modeling Earth as a sphere causes some errors to distance values. However, for sake of simplicity and efficiency, these errors are acceptable in the simulation and a spherical model is used.

Distance d to the horizon of an observer with given height h is calculated using haversine formula

$$d = \sqrt{2Rh + h^2}, \quad (5.2)$$

where R is Earth's radius. When estimating, if target is behind the horizon of radar or illuminator, the combined horizon distance of the two entities must be less than the distance between the entities.

Target must be located inside the common coverage area of radar receiver and illuminator for detection to be possible. This can be visualised as the intersection union of illuminator cov-

erage circle and radar coverage circle. The coverage circle radius is defined by the horizon distance formula (Equation 5.2).

5.5 Simulated signal processing

Overview of the signal processing scheme is:

1. If target is beyond radars horizon, discard detection candidate.
2. For each passive bistatic receiver: processes the detection candidate separately steps.
 - (a) The PBR is skipped if any the target is not inside the common coverage area, described in section 5.4.
 - (b) For each antenna in the surveillance channel:
 - i. Calculate echo signal strength (Equation 5.3).
 - ii. Calculate direct signal interference (Equation 4.8).
 - iii. If physical shielding is used, apply its effects described in subsection 5.5.2.
 - iv. If signal to interference ratio exceeds limits set by ADC dynamic range, skip this antenna (with Equation 4.10).
 - v. Combine all losses; thermal noise and other system losses defined in configuration.
 - vi. Calculate SNR, described in subsection 5.5.3.
 - vii. Calculate probability of detection from SNR value (Equation 5.5).
 - viii. Detection occurs if $P_d \geq rand[0, 1]$
 - (c) Store how many PBRs detected the target.
3. Detection happens if any of the following is true.
 - (a) If target was detected by 3 or more PBRs location can be done with triangulation.
 - (b) If target was detected by 2 PBRs and digital beamforming or direction finding (if enabled).
 - (c) With one PBR detection, can be achieved with direction finding enabled.

Having multiple antennas configured and executing signal processing to each individually is intended to simulate digital beamforming or phased array of multiple antennas feeding to

one system. Digital beamforming makes detection possible with two or more illuminators (as noted in (Malanowski, Kulpa, and Misiurewicz 2008)). Direction finding takes advantage of phased antenna array given that reception is high enough in each and reason why count of detections per antenna are stored.

5.5.1 SNR calculation

Detection candidate SNR is calculated based on radar equation echo signal component (Equation 5.3) with added integration gain G_p (Equation 4.6), reduced by total losses that are composed of noise floor (Equation 4.3) and noise power from equipment in configuration as L . These values are expressed as decibels in the results.

$$SNR = 10\log_{10}(P_r) + 10\log_{10}(G_p) - 10\log_{10}(N_r) - L \quad (5.3)$$

When calculating signal strength, the antenna gain values G_r and G_t are resolved using the antenna gain function (Equation 5.1) with azimuth and elevation values determined by target location and antenna orientation. The azimuth value is resolved by subtracting antenna orientation azimuth from target azimuth (relative to receiver or illuminator) and similarly for elevation:

$$(\alpha, \varepsilon) = (\alpha_t - \alpha_a, \varepsilon_t - \varepsilon_a), \quad (5.4)$$

where α_t and ε_t correspond to receiver-to-target (or illuminator-to-target) azimuth and elevation and α_a and ε_a to antenna orientation of receiver or illuminator.

Direct signal interference is calculated using Equation 4.8 and gain values G_t and G_r are calculated using radar-to-illuminator (and vice versa) azimuth and elevation angles, relative to antennas orientation using Equation 5.4.

5.5.2 Physical shielding

Physical shielding is direct signal suppressing technique that incoming signals are blocked with material that prevents signals from coming through. Effects of physical shielding depend on the wavelength of the signal, longer wavelengths being harder to block. For simplicity, a flat 20 dB suppression is applied to all incoming signals from direction of the associated

illuminator in a 3° wide cone. This causes targets near baseline to be less detectable.

5.5.3 Integration gain

Signal-to-noise ratio acquired from signal processing is acquired by combining the results from echo signal strength (Equation 5.3), thermal noise floor (Equation 4.3), combined system losses and processing gain from coherent integration.

Integration gain is calculated from Equation 4.6 based on the integration time defined in radar configuration. The maximum integration time limited by the cell migration is calculated from Equation 4.7.

5.5.4 Probability of detection and false alarm

Probability of detection and false alarm in the simulation is based on estimation done by (Conti et al. 2014). Using configured threshold value T_d , the calculated SNR and noise power of the radar system L , the probability of detection is defined with following function:

$$\begin{cases} P_d = e^{-\frac{T_d^2}{F(1+SNR)}} \\ P_{fa} = e^{-\frac{T_d^2}{F}}, \end{cases} \quad (5.5)$$

where T_d is detection threshold, F is noise figure (noise power) of the receiver and SNR the calculated signal-to-noise ratio. Random numbers for Java Random api are generated with Mersenne twister.

5.6 Model translation

The model was implemented in an air surveillance training simulation software as an extension to possible sensor configurations that user could create. The original software and detailed implementation of the expansion cannot be provided in this thesis and the described architecture is not complete picture of the underling system. Implementation was written in Java programming language.

6 Verification & Validation

Verifying the model is making sure that the software is built correctly, and the parts are representing the concepts intended in the design. The simulation software developed from the model was verified by examining the logging output of detection and signal processing events and comparing the results with expected outcomes defined by underlying theory (represented in section 4.2 and section 4.4).

Validating the model requires comparing the simulation execution and its behaviour against a real system (Banks et al. 2005), and in this case a real passive radar. During this research however, no access to such data was not available and validation uses the results of passive radar demonstrations described in section 4.4. In addition to realistic detection capability, the model should not consume too much system resources to be able to run in real time. The purpose of the simulation model is to be used in training simulation for air surveillance, which implies that the model should support configuration of different kinds of passive radars. Taking these three aspects, the validation should answer the following questions:

1. Does the model produce realistic results?
2. Is the model effective and simple?
3. Does the model add value?

Test scenarios for validation purposes were created with real life flight data as targets and five radar examples from section 4.4 were selected to be configured into the simulation instances. This approach was considered the best to see how well the model performs and supports building simulations for different kinds of passive radars. Since the original problem was to achieve training system model, it is essential that wide range configuration is made possible in order to explore the passive radar concept.

6.1 Target data

For first test scenario a realistic target data set was created. Realistic target data for simulations was created using the ADSB-Exchange API. The API has a function to get all flights

around a maximum of 100 nautical miles around a selected point in latitude and longitude. The API produces and returns a JSON file containing list of data of current flights in the defined area with timestamps. To produce a recording, the API was called in five second intervals to produce one hour recording with a total of 720 samples, each written in a file. Flight data had many different values and following were used to produce target paths: registration, post time, latitude, longitude, altitude, callsign and wake turbulence category (wtc).

Registration is a unique identity code given to each registered aircraft and is used to identify aircraft from data. Position information i.e. latitude, longitude and altitude is used to make target path from different samples across time given by the post time. From the target path, heading, velocity and acceleration information is estimated between the path points. Wake turbulence category were used to estimate aircraft size which greatly affects the RCS using mapping:

- 1 (small) $\rightarrow 5m^2$
- 2 (medium) $\rightarrow 40m^2$
- 3 (large) $\rightarrow 100m^2$

In total, 353 individual aircraft target paths were extracted from the file collection.

For the second test scenario, target flight paths were configured as similar as possible with the original experiment (Xie et al. 2018, Fig.9 and target Classes I, II and IV). These targets are flying at speed 200 m/s and had cruising altitudes 8000 m and 10000 m and RCS of $25m^2$.

6.2 Radar & illuminator configuration

The radar configurations in the test scenarios are based on following experiments previously mentioned in section 4.4:

- PaRaDe-2 tested in (Malanowski et al. 2012) and described in (Malanowski, Kulpa, and Misiurewicz 2008).
- Multistatic configuration of two PBRs described in (Xie et al. 2018).
- DVB-T based passive radar developed at St. Petersburg electrotechnical university

(Vorobev, Barkhatov, and Kutuzov 2017)(Barkhatov, Vorobev, and Konovalov 2017).

- DVB-T passive radar from Warsaw University (Płotka et al. 2020).

Configurations of passive bistatic radars tested in simulation scenarios are described in Table 3. Illuminators for respective PBRs are found from Table 4. Reference value for transmission gain of DVB-T transmitter is from (ITU 2016) and yagi antenna radiation pattern reference can be examined from (Viezbicke 1976). Each passive bistatic radar (PBR) was configured to process detection events in 4 second intervals.

The first test scenario used radars PBR 1, 2, 3, 4 and 5, with targets from recorded 1 hour flight data from ADS-B Exchange. The first test scenario was executed in three runs first with seed number 1 and then randomly chosen seeds, 2204 and 4798 to verify randomization.

Second test scenario was created following more accurately the experiment setting in (Xie et al. 2018). This test used radars PBR 6, 7 and 8 are used in this scenario. Illuminators T6 and T7 are located in a same site, but are used as individual illuminator-receiver pairs with PBR6 and PBR7. The configuration is intended to better reflect similar conditions in the experiment carried out as in test 1.

Third test scenario is a recreation of the first test scenario with changes to PBR 1 and PBR 5, which were labeled PBR 9 and PBR 10 respectively. Target scenario is same with corrected RCS functionality and half the duration.

label	DF	DBF	PS	F	T_d	DR	T_i	T_k	T_x	Antenna
PBR 1	No	Yes	No	1 dB	10 dB	144 dB	1.0 s	300 K	T1	Table 5
PBR 2	No	Yes	No	1 dB	10 dB	144 dB	1.0 s	300 K	T2	Table 5
PBR 3	No	Yes	No	1 dB	10 dB	144 dB	1.0 s	300 K	T3	Table 5
PBR 4	Yes	Yes	No	1 dB	10 dB	96 dB	0.273 s	300 K	T4	Table 6
PBR 5	Yes	No	No	0 dB	10 dB	96 dB	1.0 s	300 K	T5	Table 7
PBR 6	No	Yes	No	3 dB	10 dB	96 dB	1.0 s	300 K	T6	Figure 15
PBR 7	No	Yes	No	3 dB	10 dB	96 dB	1.0 s	300 K	T7	Figure 15
PBR 8	No	Yes	No	3 dB	10 dB	96 dB	1.0 s	300 K	T8	Figure 15
PBR 9	Yes	No	No	3 dB	10 dB	144 dB	1.0 s	300 K	T1	Figure 15
PBR 10	Yes	No	No	3 dB	10 dB	96 dB	0.2 s	300 K	T9	Table 7

Table 3. Radar configurations in the test scenarios.

label	f_c	P_t	B	Gain	Baseline	height
T1	98 MHz	60 kW	150 kHz	0 dB	60 km	150 m
T2	98.6 MHz	3 kW	150 kHz	0 dB	14 km	100 m
T3	97 MHz	3 kW	150 kHz	0 dB	37 km	100 m
T4	650 MHz	5 kW	8 MHz	10 dB	49 km	120 m
T5	550 MHz	10.4 kW	8 MHz	10 dB	27 km	100 m
T6	102.6 MHz	3 kW	150 kHz	0 dB	37.7 km	200 m
T7	97.0 MHz	3 kW	150 kHz	0 dB	37.7 km	200 m
T8	98.6 MHz	3 kW	150 kHz	0 dB	14.1 km	200 m
T9	550 MHz	10.4 kW	8 MHz	10 dB	27 km	100 m

Table 4. Illuminator configurations in the test scenarios.

0°	30°	60°	300°	330°	360°
0 dB	-3	-30	-30	-3	0

Table 5. Gain table of a single antenna element used in PaRaDe (PBR 1, 2 and 3).

0°	30°	50°	180°	310°	330°	360°
24	10	3	0	3	10	24

Table 6. Gain table of surveillance antenna array used in the PBR 4.

0°	30°	90°	180°	270°	330°	360°
8	5	-32	-7	-32	5	8

Table 7. Gain table of the 4 element yagi antenna used in the PBR 5.

Configuration tables of the second test run.

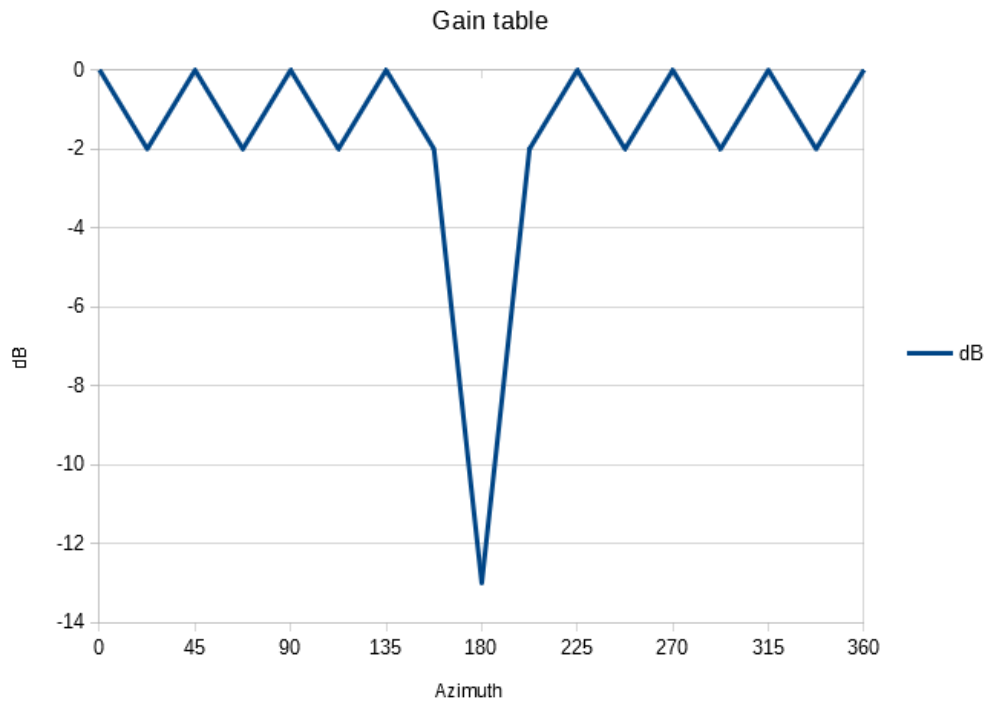


Figure 15. Radiation pattern of antenna used in PBR 6, 7 and 8.

7 Results

Section 7.1 goes through verification and validation analysis results. Section 7.2 covers problems in the model that were revealed during simulation development and testing with suggestions to solve these problems. Finally in section 7.3 improvements are made to model from suggestions.

7.1 Test simulation analysis

7.1.1 First test scenario

From a total of 1,664,871 detection events, there were 989,231 cases where the execution continued to signal processing phase and were not suppressed by *beyond the horizon* case. Figure 16 shows an overview of the whole scenario. Target paths are shown in black, radar receivers are all located in same place at the origin, illuminators are marked with their labels.

Due to mistake in programming, the WTC to RCS mapping was not done to targets and all targets in scenario 1 were processed with hard coded RCS value of $5m^2$. This was fixed for the test scenarios 2 and 3.

Figure 17 shows a comparison of cumulative distribution for SNR to probability of detection, where solid line represents theoretical assumption (Equation 5.5 with threshold value of 10 and 1 dBm noise power) and dashed represents simulation results. This verifies that the developed simulation software works as intended by producing detections in correct proportion based on SNR. Simulation result SNR to Pd was calculated by collecting a histogram from smallest recorded SNR value -30 dB and largest value 70 dB with 1 dB step size using Pandas. This procedure was done for all three test runs to verify that there was no major difference to this with variable seed numbers.

To verify correct calculation for SNR in detection scenarios, a random set of detection events were selected to verify that the target maneuver parameters along with radar and illuminator configuration should produce correct values to variables used to calculate SNR (described in subsection 5.5.1). When comparing SNR calculation from output to the theory there was

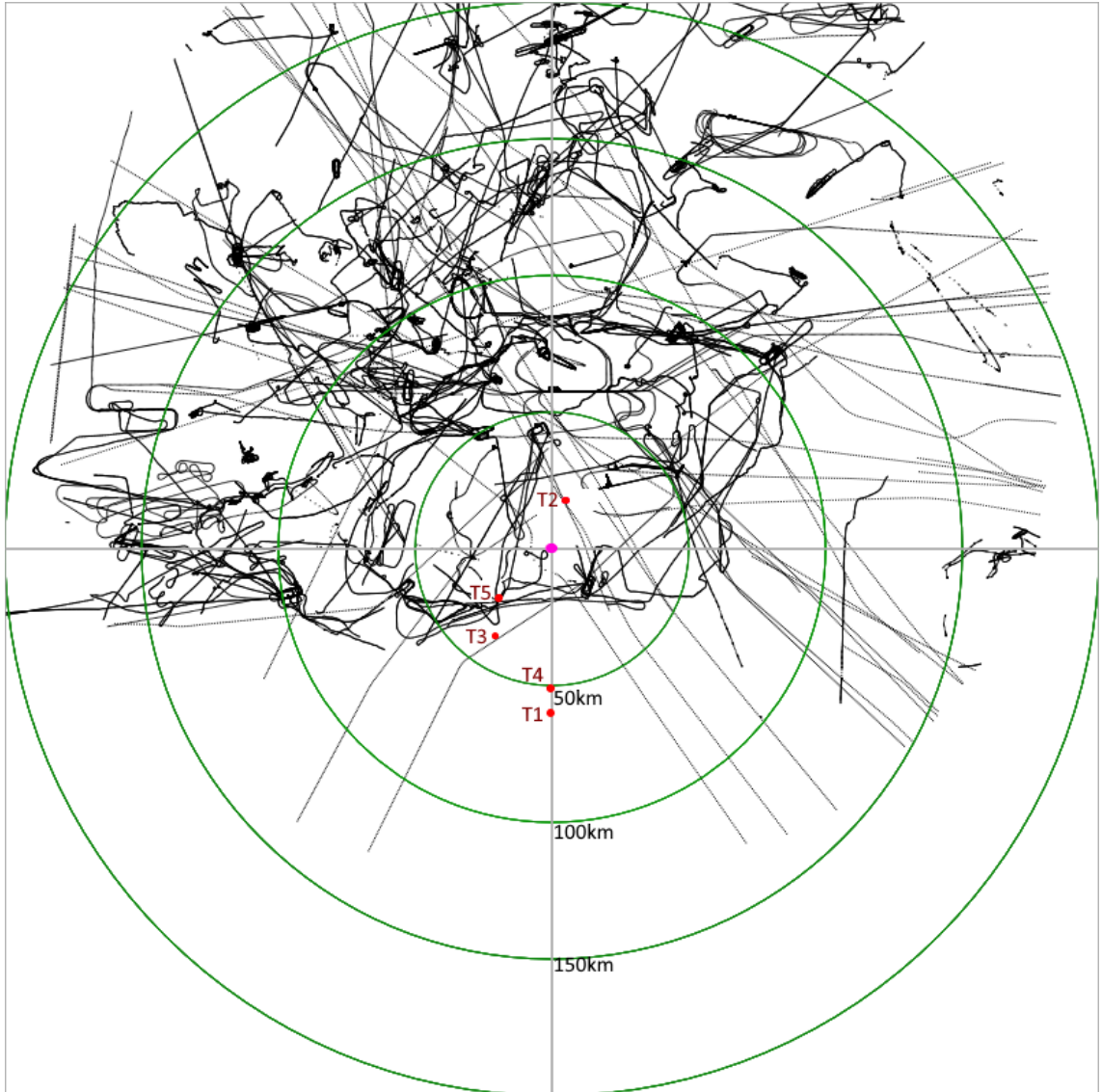


Figure 16. Overview of first simulation run setup.

some errors in loss calculations: loss from antennas should have been added to the total noise power of the radar, but it was not in the logging output. This information is not in the configuration tables and is hidden in the antenna configuration.

For example, consider following random sample:

- R_r : 16003.7521530279 m
- R_t : 51241.2125337998 m
- P_t : 60,000W = 60,000,000 mW
- Bandwidth: 150 kHz
- λ : 3.05910671428571 m
- RCS: $5m^2$
- T_{max} : 1s
- G_r : -30 dB = 0.001
- G_t : 0 dB = 1
- F: 1 dB
- L: 1 dB (from antenna)

According to the simulation log, this should produce 26.0568355394546 dB SNR.

To verify this, we calculate integration gain (Equation 4.6), received signal strength (Equation 5.3) and noise floor (Equation 4.3) (in decibels):

$$\begin{aligned}
 G_i &= 10\log_{10}(1s \cdot 150000) && \approx 51.761dB. \\
 P_e &= 10\log_{10}\left(\frac{60000000 \cdot 0.001 \cdot 1 \cdot 3.0591^2 \cdot 5^2}{(4\pi)^3 \cdot (16003)^2 \cdot (51241)^2}\right) && \approx -145.77dB \\
 p_n &= 10\log_{10}\left(\frac{1}{1.38064852 \cdot 10^{-23} \cdot 150000 \cdot 1000}\right) && \approx -122.07dB \\
 SNR_{dB} &= P_e + G_i - P_n - F - L && \approx 26.06dB
 \end{aligned}$$

These values corresponds to those found in simulation result log.

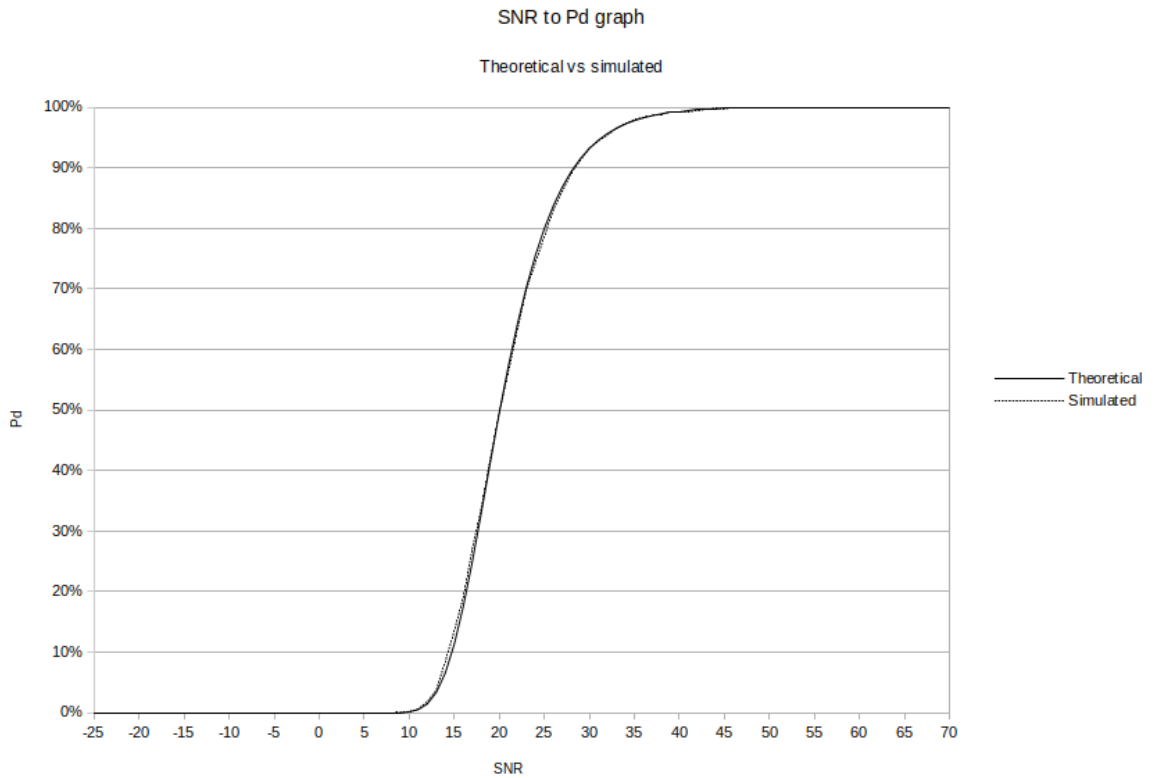


Figure 17. Comparison of SNR to Pd value between simulation results and theoretical assumption.

A best effort attempt to validate the model is done by comparing detection performance with targets that are somewhat similar to scenarios described in the literature.

PBR 1

This radar was reported in (Malanowski et al. 2012) to detect airliner from monostatic equivalent range of 285 km. In the simulation scenario, longest detected range was 245 km of a target with $5 m^2$ RCS. The events at that range for the target had 17.7% and with 4 second reporting period would yield at least one detection in every 60 seconds with approximately 95% certainty, which would be a noticeable rate. Target in the reported experiment is probably larger in RCS as in the simulation.

However, simulation comes quite close to producing similar results as in the experiment. It is also important to notice that in the experiment, confirmations on target location were done

using ADS-B. Similarly in the simulation, two or more radars would be needed to locate the target. Assuming location could be determined, Figure 18 show detections of few selected targets from scenario.

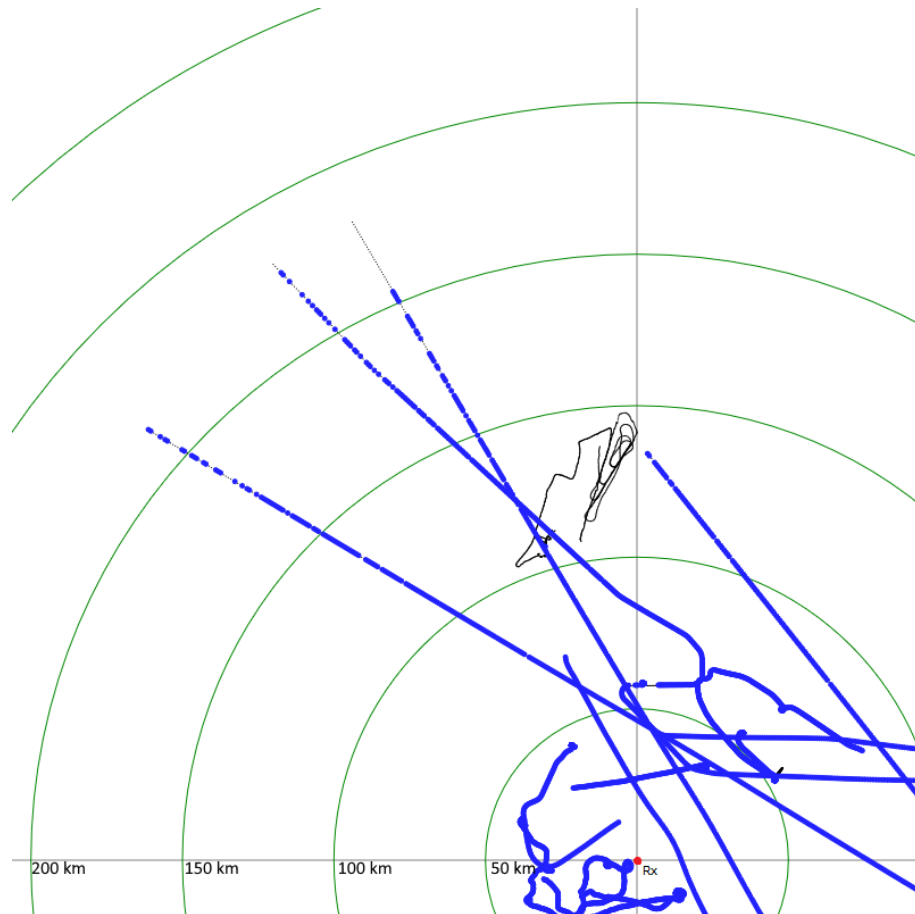


Figure 18. PBR 1 detections of few selected targets.

PBR 2 & PBR 3 in multistatic configuration

This radar was based on (Xie et al. 2018) with two illuminators and similar antenna configuration as PBR 1, where target detection along with location requires two detections from both bistatic radars. When looking for for maximum detection range, there were some occasional such detections from a maximum of 122 km, however since the probability of detection is around 19% for PBR 2 and 16% for PBR 3 at that range, getting two detections inside same event is 3.2%.

Reported in the original experiment, the radar successfully tracks aircraft from monostatic

range of 60 km. When examining detection of targets inside 59-61 km range area, for PBR 2 instance detection probabilities were 85% and PBR 3 80% on average, which is 68% when considering combined detection. The SNR (and therefore Pd) is of course affected by bistatic range ($R_r + R_t$) and not monostatic range (R_r) alone but for simplicity monostatic range evaluation is considered. From these results the simulation at least partly reflects the performance of the original experiment.

Detection range in simulation extends beyond reported in the experiment, as it can be seen from Figure 19 It might be due to lower dynamic range of the analog to digital converter in the experiment system. ADC dynamic range is a major limiting factor in passive radars.

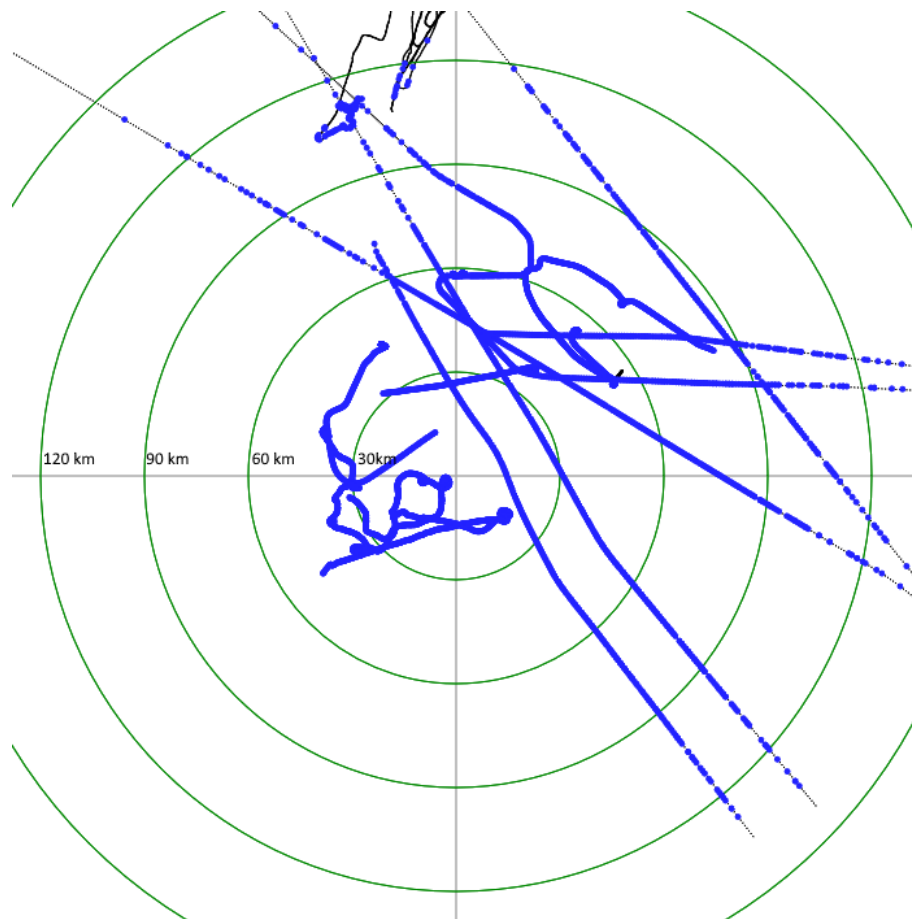


Figure 19. PBR 2 and PBR 3 detections of few selected targets.

When targets are near the transmitter-receiver baseline, the accuracy of range measurement is not unstable, as it should be compared to the original results of experiment. Generally

range resolution is not taken in account in the processing scheme currently. This is design oversight is a clear handicap in model accuracy validity.

PBR 4

The experiment reported measured SNR of 20 dB when a Cessna aircraft was flying in 41 km target-to-receiver range and 91 km transmitter-to-receiver range. Simulation results with similar conditions lead to an average SNR of 38 dB which is significantly higher. Possible explanations for such difference might be found from different size of airplane and clutter effect from ground reflections not taken in account in the simulation model.

Figure 20 demonstrates how the very high gain antenna pattern is affecting the detection range at the 30° beam towards north, where it was configured to point. This simulation has good detection range up to ≈ 135 km. It can be noted here too, that the ADC dynamic range limits the detection range greatly.

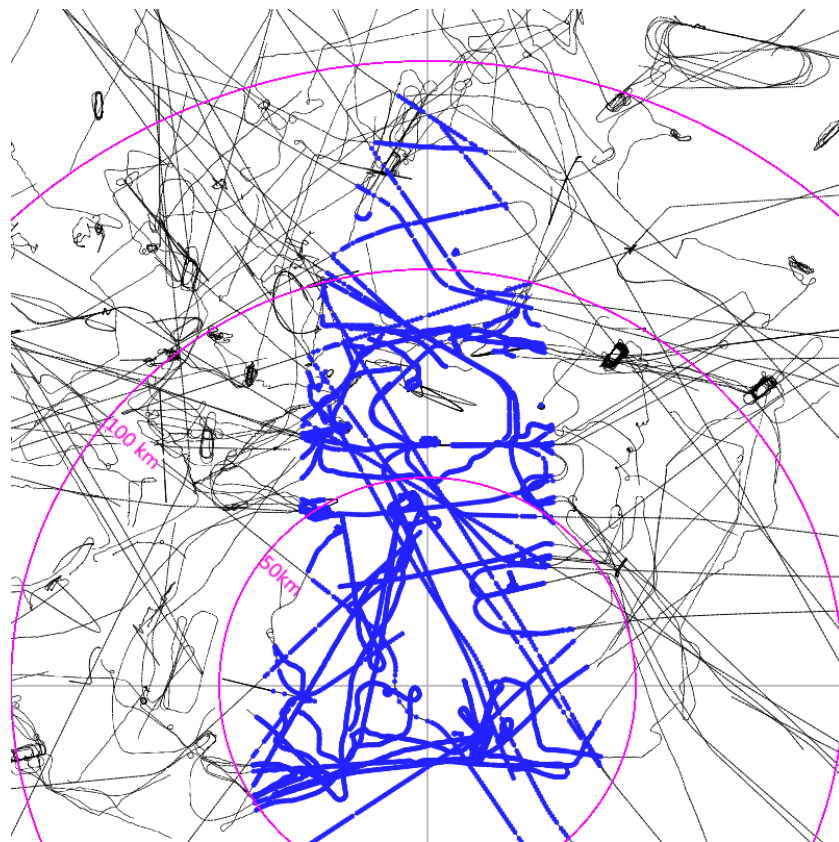


Figure 20. PBR 4 detections of all targets.

PBR 5

This radar was mistakenly configured with incorrect integration time, carrier frequency and effective bandwidth in the first test scenario. The intended configuration from the original research was implemented in third scenario, which is analysed in subsection 7.1.3.

7.1.2 Second test scenario

Results of the simulation are shown in Figure 21 and for comparison the original results (Xie et al. 2018, fig.9). Thin black line represents the flight path of the target and blue dots are detections by radar. Radar is located at the origin and labeled as "Rx" and illuminators labeled as "Tx".

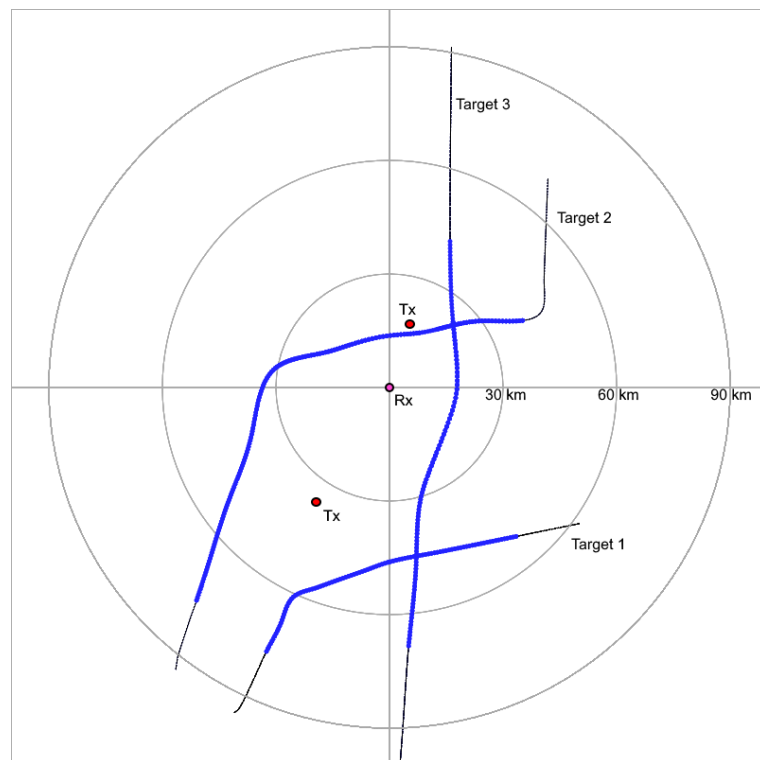
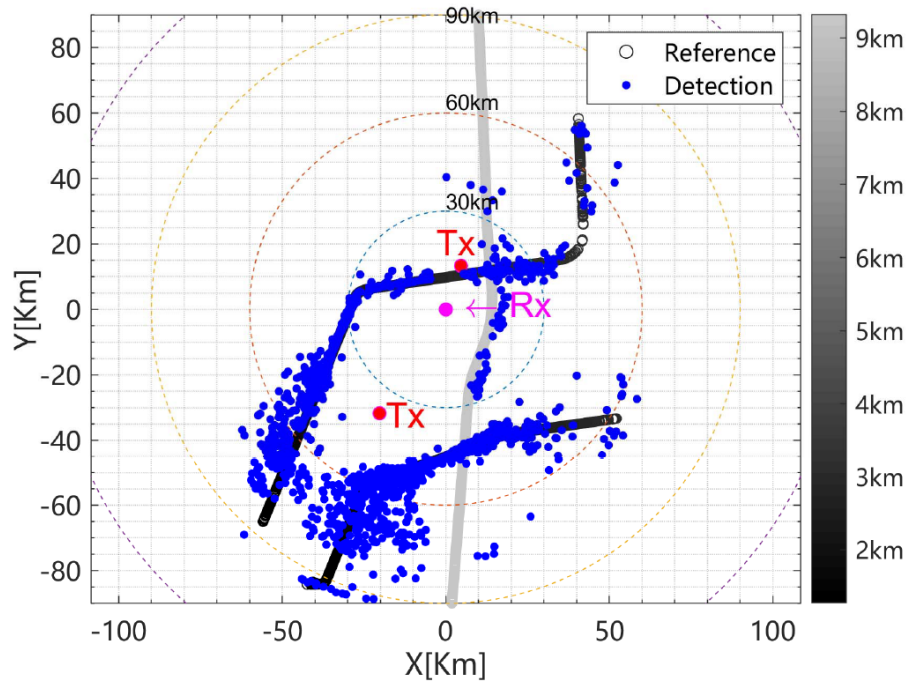


Figure 21. Detection results of second test scenario.



© 2018 IEEE

Figure 22. Comparison to results of (Xie et al. 2018).

The two figures demonstrate the lack of any range measurement errors in the simulation execution and therefore they are perfectly on the flight path. When considering range limits, the simulation seems to better job at modeling the detection range of the original radar in this case. The maximum range is very similar and detections in the simulation begin to show closely in cases where the original radar produces plots in high density. One of the targets (no.3), which is flying the highest in original case, is clearly detected with better performance in simulation. In the simulation scenario, the SIR was the major limiting factor for maximum detection range.

7.1.3 Third test scenario

PBR 9

In this scenario, the target RCS calculation worked correctly and some targets got much larger as it can be seen from Figure 23. The situation is similar to PBR 1, but here Target

1 RCS is $40 m^2$ and Target 2 RCS is $100 m^2$. Target 2 is detected with more density on the blue plots. Compared to the results shown for PBR Figure 18, this one is clearly detecting these large targets better, as it should. The simulation seems to follow quite closely to the (Malanowski et al. 2012), however more experiments are needed.

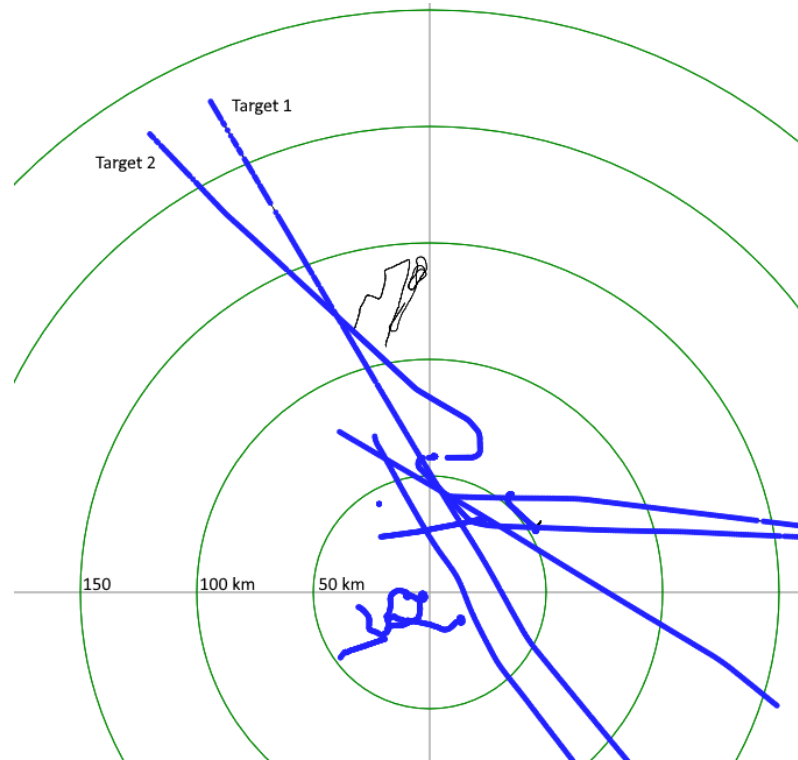


Figure 23. PBR 9 detections of few selected targets.

PBR 10

When looking at the detections made by the radar (Figure 24), this VHF DVB-T based radar seems to have same problems as PBR 4. The detection range far exceeds the results of original experiments. One possibility for very high SNR values in simulation compared to original might be difference in rule of thumb approach for integration gain in digital versus analog systems. Future research is required for accurate DVB-T based passive radar simulations.

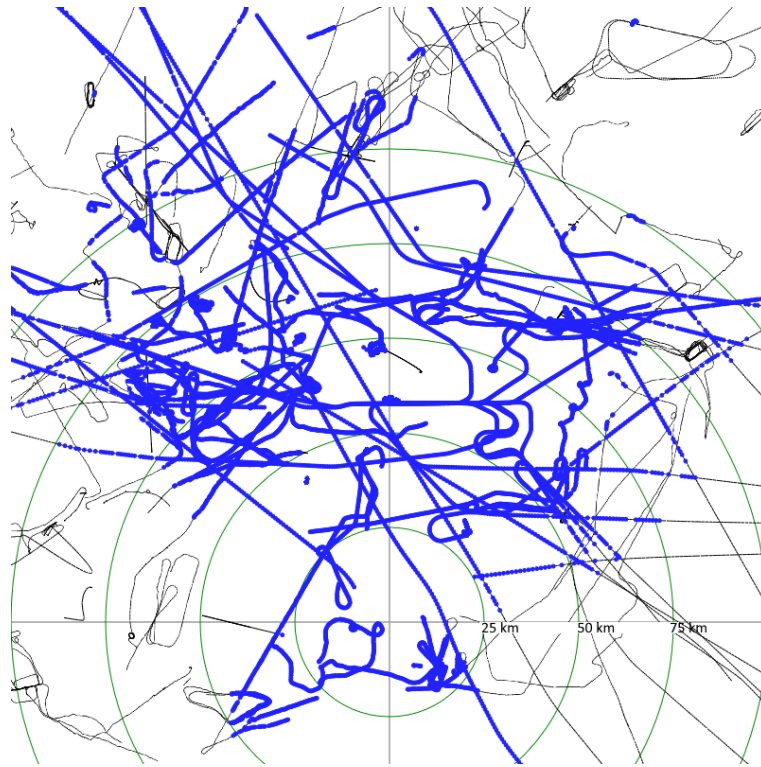


Figure 24. PBR 10 detections of all targets.

7.2 Problems and suggestions

The software implementation of the initial model did not make any use of the reference channel antenna configuration, so it is redundant. For more complex simulations, the reference channel antenna configuration might be useful. For example, there could be more sophisticated simulation scenarios with jamming or other interference sources that could affect reference channel but not surveillance channel.

In the current model implementation, configuring multiple antennas just to simulate phased antenna array or digital beamforming is unnecessarily complex. Just one antenna with accurately defined antenna pattern would be sufficient. Direction finding and digital beamforming attributes describe how many bistatic detections are required for accurate detection. Having multiple antennas in architecture could be useful when implementing more accurate simulations in the future, but for current design it is unnecessarily complex.

Complexity of configuring the radiation pattern reduces the intended *simple* usability. Ele-

vation values do not vary as much as azimuth values and when it does, the target is usually very close to the radar and effect on antenna gain is significantly lower compared to range. However, antenna gain is an important aspect of the parameters that affect the radar performance and the gain table model allows experimentation and increases accuracy of the model. Increasing usability of radiation pattern table configuration would require additional application with effective tools for graphing and plotting into a table.

Illuminator configuration instances were limited to one per target instance, which caused problems when configuring larger scenarios with multiple types of illuminators in same location. Initial model would require several identical target definitions if multiple kind of illuminators were desired to be use. Solution to problem is to define illuminator instances as an array and configure target reference and illuminator index to PBR configuration.

It is has been previously noted that content of the program has drastic effects on the effective bandwidth, which affect significantly to performance prediction when considering integration gain. This was not taken into account in the first model and further improvements would benefit from bandwidth fluctuation modeling research to have more accurate representation of performance.

Range resolution is not visible in the simulation reports which is clearly showing when comparing to test scenario of (Xie et al. 2018), where plots get very scattered at times. FM radio based passive radars have range resolution of 2 to 3 km and current model produces accurate position estimates with arbitrary precision, which is a clear design oversight. Researching the effects of range resolution to target location estimation in passive radar simulation is proposed as important suggestion to improve the model.

False positive detection generation design was overlooked in this simulation due to limited scope of the available resources. A simple probabilistic model for generating false detections in range cells using the probability of false alarm calculation (Equation 5.5) could be a beginning step to approach this issue.

It is clear, that the simulation model cannot be adequately validated. However, an effort was made to clarify that what needs to be done in order to validate the developed model and how setup for validation is easily carried out.

7.3 Improved model

As a result from problems encountered, improvements were made to the model that are presented in Figure 25. The reference channel was removed as unnecessary and replaced with the illuminator target reference since it actually contains the important information. It is reasonable to assume that the signal strength from illuminator to receiver reference channel is good. List of antenna arrays of surveillance channel was reduced to a single instance to reduce complexity of the configuration. Although it is viable as List too, since it is ultimately developers choice to make support for complex multiple antenna simulations. Variable names were adjusted to be more descriptive in general, however it is always up to developer to name variables descriptively.

For the signal processing scheme, there are two functionalities to modify: First, there is no need to loop trough any antennas and antenna is used as is. Second, the concept of physical shielding does not necessarily mean that it affects the surveillance channel, so it is replaced with the generic DSI suppression using the value *DSICancellation* in dB.

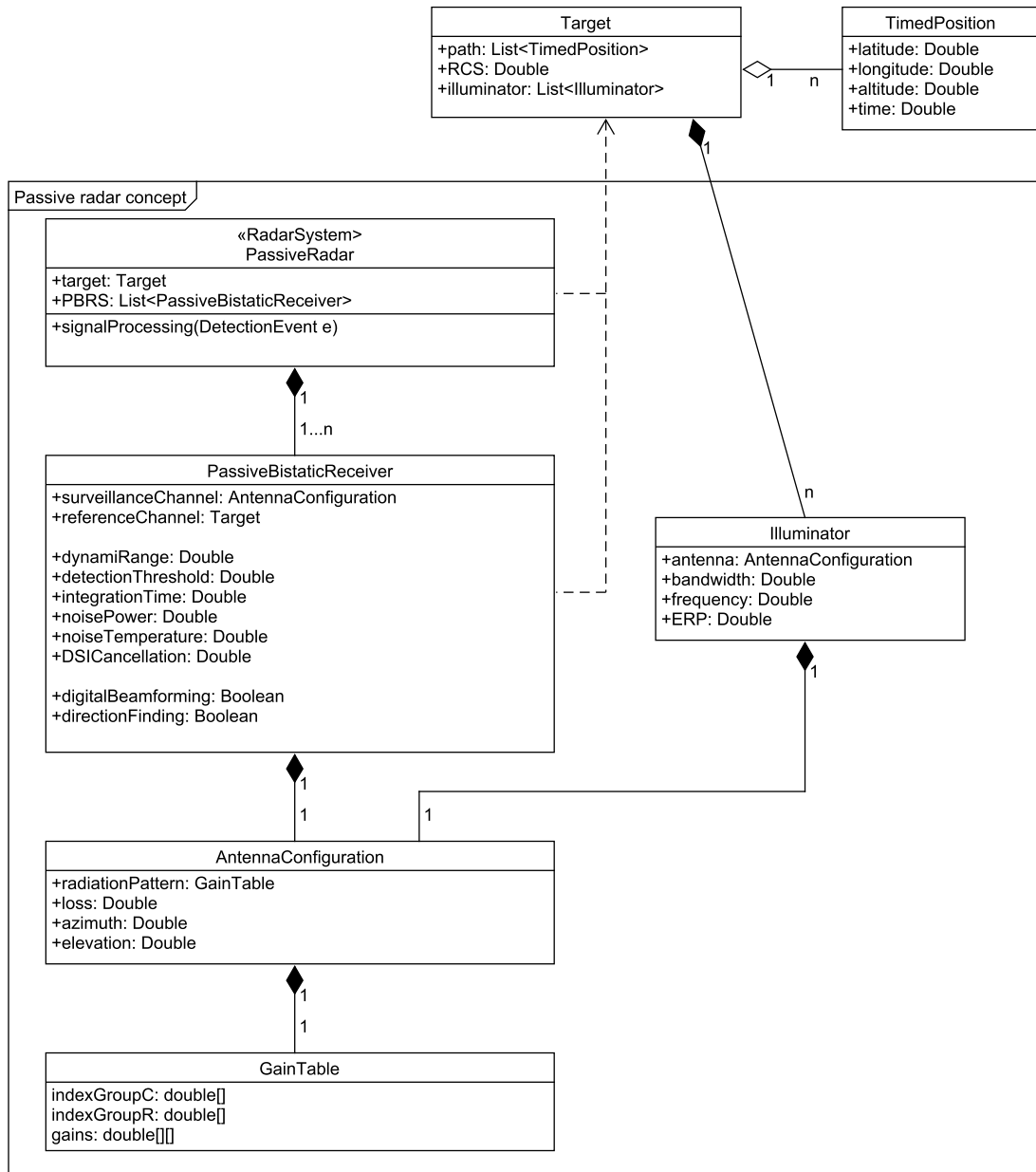


Figure 25. Improved model based on suggestions.

8 Conclusion

In this research, a design and construction of passive radar simulation for real time application purposes was studied. A theoretical ground was given by literature review of old and modern passive bistatic radar demonstrations in research.

To answer the original research question (*how to model a passive radar for real-time simulation?*), a model concept was created that represents passive radar components in UML notation and a simulated signal processing scheme was developed using the abstract model as a guideline. Using the model as a guideline, an extension to an air surveillance training system was implemented that simulates passive radar in bistatic and multistatic configurations. Problems encountered during implementation of the model application were documented and suggestions for future improvements provided. Considering that the developer of the model is not an expert in radars, the model succeeds to support fairly accurate simulation of FM based passive radars demonstrated in (Malanowski, Kulpa, and Misiurewicz 2008), while being easy to configure. DVB-T based simulation was not successful in this simulation. Also range resolution and false detection design were overlooked. From these results, author of this paper proposes the model concept described in chapter 5 as an effective starting point of passive radar simulation model development.

From the evidence in literature, alone a comprehensive comparison between simulation results and detection results of passive radar demonstrators cannot be done. Validating the simulation requires a setup with real passive radar accompanied with ADS-B based locating or a co-operative target to record performance of the radar with high time resolution. That scenario configured into the simulation would yield much more accurate results.

Topics of future for further improvements for the model: 1) Target fluctuation models in passive bistatic radars for simulation. 2) Developing models to simulate variety in effective bandwidth of FM radio illuminators with different broadcast content. 3) Simulating effects of range resolution in passive radar target location methods. 4) Real-time simulation signal processing scheme for DVB-T based illuminators.

Bibliography

521-1984, IEEE Std. 1984. *IEEE Standard Letter Designations for Radar-Frequency Bands*. IEEE.

Admiralty Manual of Navigation. 1987. Ministry of Defence (NAVY).

Banks, Jerry, John S. Carson II, Barry L. Nelson, and David M. Nicol. 2005. *Discrete-Event System Simulation*. Prentice Hall, Inc.

Barkhatov, A., E. Vorobev, and A. Konovalov. 2017. "Experimental Results of DVB-T2 Passive Coherent Location Radar". *2017 IEEE Conference of Russian Young Researchers in Electrical and Electronic Engineering (EIConRus)*. doi:10.1109/EIConRus.2017.7910784.

Barott, William C., Ted Dabrowski, and Braham Himed. 2015. "Fidelity and Complexity in Passive Radar Simulations". *IEEE Computer Society*. doi:10.1109/HASE.2015.30.

Brown, James. 2013. *FM Airborne Passive Radar*. UCL Discovery. https://discovery.ucl.ac.uk/id/eprint/1397756/4/JBrown_Airborne_Passive_Radar.pdf.

Conti, M., C. Moscardini, A. Capria, and R. Soleti. 2014. "Estimation of Passive Bistatic Radar Detection Probability: Experimental Results". *2014 11th European Radar Conference*. doi:10.1109/EuRAD.2014.6991223.

Digita. 2020. "Taajuudet | Digita". Visited on January 2020. <https://www.digita.fi/antennitv/vapaat-kanavat-ja-vastaanotto/hyodyllista-tietoa-tvsta/taajuudet/>.

Griffiths, H.D., and C.J. Baker. 2005. "Passive coherent location radar systems. Part 1: Performance prediction". *IEEE Proceedings online* 152 (3): 153–159. doi:10.1049/ip-rsn:20045082.

Griffiths, Hugh D., and Christopher J. Baker. 2017. *An Introduction to passive radar*. Artech House. ISBN: 978-1-63081-036-8.

- Griffiths, Hugh, and Nicholas Willis. 2010. "Klein Heidelberg - The First Modern Bistatic Radar System". *IEEE Transactions on Aerospace and Electronic Systems*: 1571–1588.
- Guo, Woodbridge, and Baker. 2008. "Evaluation of WiFi Beacon transmissions for wireless based passive radar". *2008 IEEE Radar Conference*. doi:10.1109/RADAR.2008.4720810.
- ITU. 2016. "Characteristics of digital terrestrial television broadcasting systems in the frequency band 470-862 MHz for frequency sharing/interference analysis". Visited on 2016. https://www.itu.int/dms_pub/itu-r/opb/rep/R-REP-BT.2383-1-2016-PDF-E.pdf.
- Malanowski, M., K.S. Kulpa, P. Samczynski, J. Misiurewicz, and J. Kulpa. 2012. "Long range FM-based passive radar". *IET International Conference on Radar Systems (Radar 2012)*. doi:10.1049/cp.2012.1578.
- Malanowski and Kulpa. 2008. "DIGITAL BEAMFORMING FOR PASSIVE COHERENT LOCATION RADAR". *MRRS-2008 Symposium Proceedings*.
- Malanowski, Kulpa, and Misiurewicz. 2008. "PaRaDe – Passive Radar Demonstrator Family Development at Warsaw University of Technology". *MRRS-2008 Symposium Proceedings*.
- Melvin, Scheer. 2014. *Principles of Modern Radars: Volume III: Radar Applications*. SciTech Publishing.
- O'Hagan, Colone, Baker, and Griffing. 2007. "Passive Bistatic Radar (PBR) Demonstrator". *IET International Conference on Radar Systems*: 1–5.
- P.E.Howland. 2008. "Target tracking using television-based bistatic radar". *IEE Proceedings online no. 19990322*. doi:10.1049lip-rsn:19990322.
- Palmer, Palumbo, Van Cao, and Howard. 2009. "A new Illuminator of Opportunity Bistatic Radar Research Project at DSTO". *Defence Science and Technology Organisation*.
- Pető, Tamás, Rudolf Sella, Levente Dudás, and Péter Renner. 2014. "Digital Television Broadcast -Based Passive Radar Research and Development". *20th International Conference on Microwaves*: 1–4.

- Petri, Berizzi, Martorella, Dalle Mese, and Capria. 2010. "A Software Defined UMTS Passive Radar Demonstrator". *11th International radarsymposium*: 1–4.
- Plotka, M., M. Malanowski, P. Samczyński, K. Kulpa, and K. Abratkiewicz. 2020. "Passive Bistatic Radar Based on VHF DVB-T Signal". *2020 IEEE International Radar Conference (RADAR)*. doi:10.1109/RADAR42522.2020.9114859.
- Pölönen and Koivunen. 2013. "Control Symbol Based Fluctuating Target Detection in DVB-T2 Passive Radar Systems". *2013 IEEE Radar Conference (RadarCon13)*. doi:10.1109/RADAR.2013.6586076.
- Qing Wang, Chunping Hou, and Yilong Lu. 2010. "An Experimental Study of WiMAX-Based Passive Radar". *IEEE TRANSACTIONS ON MICROWAVE THEORY AND TECHNIQUES* 58 (12): 3502–3510.
- R. Timothy Hitchcock, CLSO, CIH. 2004. *Radio-Frequency and Microwave Radiation: Third edition*. American Industrial Hygiene Association.
- Satar, Baris, Yetkin Ersoy, Gokhan Soysal, and Murat Efe. 2018. "A Do It Yourself Mobile Communications Signal Based Passive Radar". *21st International Conference on Information Fusion (FUSION)*.
- Skolnik, Merrill I. 2001. *Introduction to radar systems: Third edition*. McGraw-Hill.
- Sun, Honbo, Danny K.P. Tan, and Yilong Lu. 2008. "Aircraft Target Measurements Using A GSM-Based Passive Radar". *2008 IEEE Radar Conference*. doi:10.1109/RADAR.2008.4721053.
- Swerling, Peter. 1954. "Probability of Detection for Fluctuating Targets".
- Takeda, Hidekai, Paul Veerkamp, Tetsuo Tomiyama, and Hiroyuki Yoshikawa. 1990. "Modeling Design Processes". *AI Magazine* 11 (4): 37–48. doi:10.1049/ip-rsn:20045082.
- Vaishnavi, Vijay, Bill Keuchler, and Stacie Petter. 2019. "DESIGN SCIENCE RESEARCH IN INFORMATION SYSTEMS". Visited on June 30, 2019. <http://www.desrist.org/design-research-in-information-systems/>.

- Viezbicke, Peter P. 1976. *Yagi antenna design*. NATIONAL BUREAU OF STANDARDS. <https://tf.nist.gov/general/pdf/451.pdf>.
- Vorobev, E., A. Barkhatov, and V. Kutuzov. 2017. “DVB-T2 Passive Coherent Location Radar”. *2017 IEEE Conference of Russian Young Researchers in Electrical and Electronic Engineering (EIconRus)*. doi:10.1109/EIconRusNW.2016.7448224.
- Vorobev, E., A. Barkhatov, V. Veremyev, and V. Kutuzov. 2018. “DVB-T2 Passive Radar Developed at Saint Petersburg Electrotechnical University”. *2018 22nd International Microwave and Radar Conference (MIKON)*. doi:10.23919/MIKON.2018.8405178.
- Xianrong, Zhixin, Zhang, and Qihong. 2011. “HF Passive Bistatic Radar Based on DRM Illuminators”. *Proceedings of 2011 IEEE CIE International Conference on Radar*. doi:10.1109/CIE-Radar.2011.6159499.
- Xie, Deqiang, Jianxin Yi, Ji Shen, and Xianrong Wan. 2018. “Experimental Research of Multi-FM Based Passive Radar”. *2018 12th International Symposium on Antennas, Propagation and EM Theory (ISAPE)*. doi:10.1109/ISAPE.2018.8634281.
- Yannopoulou, Nikolitsa, and Petros Zimourtopoulos. 2011. “Dipole Antenna Radiation Pattern”. Visited on 2021. <https://demonstrations.wolfram.com/DipoleAntennaRadiationPattern/>.
- Zywek, Malanowski, and Baczyk. 2016. “A Signal and Plot Simulator for Passive Bistatic Radar”. *2016 17th International Radar Symposium (IRS)*. doi:10.1109/IRS.2016.7497373.